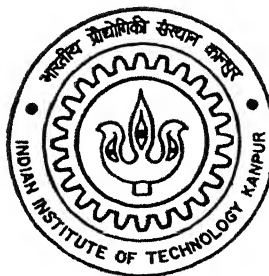# ELECTRODEPOSITION OF Ni-WC COMPOSITE COATING

By

Maddela Surender

DEPARTMENT OF MATERIALS AND METALLURGICAL ENGINEERING

Indian Institute of Technology Kanpur

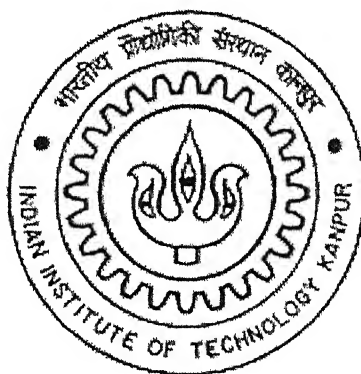### JULY, 2003

ELECTRODEPOSITION OF Ni-WC COMPOSITE COATING

A Thesis submitted

In Partial Fulfillment of the Requirements for the Degree of

MASTER OF TECHNOLOGY

by

MADDELA SURENDER (Y120611)

to the

DEPARTMENT OF MATERIALS AND METALLURGICAL ENGINEERING

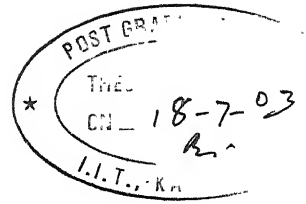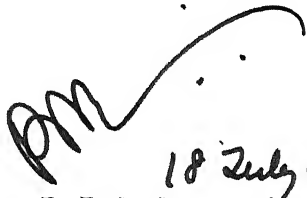**INDIAN INSTITUTE OF TECHNOLOGY, KANPUR-208016 INDIA.**

JULY 2003

CERTIFICATE

This is to certify that the work contained in the thesis entitled **"ELECTRODEPOSITION OF Ni-WC COMPOSITE COATING"** by *M. Surender* (Roll No. Y120611) has been carried out under supervision and to the best of our knowledge this has not been submitted elsewhere for a degree.

18 July 03

Dr. R. Balsubramaniam

Professor

Materials and Metallurgical Engineering

Indian Institute of Technology-Kanpur

Kanpur, India 208016.

Dr. Bikramjit Basu

Assistant Professor

Materials and Metallurgical Engineering

Indian Institute of Technology-Kanpur

Kanpur, India 208016.

ACKNOWLEDGMENTS

At the first out set, I would like to express my sincere gratitude for the expert guidance given by my guru and one of my thesis supervisors Prof. R. Balasubramaniam. The technical knowledge obtained from him during this tenure is precious and should be acknowledged with highest priority.

I am in great debt for the continuous encouragement and able guidance given by my other young and dynamic supervisor Dr. Bikramjit Basu. I highly acknowledge him especially for various fruitful discussions regarding the evaluation of friction and wear part of my thesis.

My life has not got molded to this shape without the continuous direction and supervision of Dr. J. Viplava Kumar. Whatever I am today is because of the driving force given by him in understanding the technical and general concepts through out my entire life and I am highly indebted to him. I also take this opportunity to acknowledge Sri K. Ramesh and Sri R.Venkat for their precious suggestions whenever necessary.

I express special thanks to Prof. S. Bhargav, Head of the Department, MME for giving his kind permission to carry over this work without which this could not be possible.

I wish to express my sincere appreciation of valuable help and suggestions obtained from Dr.M.N.Mungole. Special thanks to him for providing all possible helps regarding consumables, laboratory accessibility and technical know-how.

I am thankful to B V Manoj Kumar, P. Suresh Babu, Shaik Imam, Sunil and Rajasekhar for the rejuvenation obtained in their company through out this period without which the work would not have progressed. Thanks are due to all my friends and my lab colleagues who have helped me in various capacities. Prominent amongst them are Shankar, Laha, Abhishek, Animesh, Shriram and Mishra, Murthy, Ravi…. The list goes on and is in no means exhaustive.

I take this opportunity to express my thanks to Harish Varma for his timely help in experiment related work.

Last but not the least, at this time, I would like to express my deep sense of gratitude to my beloved parents and my family members for their immense patience, moral support, courage and inspiration during this research programme.

M. Surender

Contents

ABSTRACT

In the present work, the processing and properties of electrodeposited metal-matrix composite coating based on Ni-WC system is investigated. WC particles with average size of 5 μm were co-deposited with Ni using Watts' bath, with the WC particles well suspended in the electrolyte. The effect of the plating variables (current density and temperature) was initially studied. The weight percentage of WC in the deposited layer decreased with increasing current density from 0.1 to 0.3 A/cm^2 and this was confirmed by microhardness measurements. Electrochemical polarization tests were performed on the Ni-WC coated composites and on pure Ni. The potentiodynamic polarization behaviour of the coated samples was compared with that of pure Ni in 0.1 mol/l sulfuric acid solution. The passive current density increased and the passive range decreased in the case of the coatings compared to pure Ni. The friction and wear resistance of the electrodeposited Ni-WC composite coatings were studied using a small amplitude reciprocating friction wear tester and compared with the wear resistance of base mild steel and pure Ni. The wear resistance improved with increasing WC content in the composite. The embedded WC particles impede the wear process resulting in a lower coefficient of friction (COF) when compared with pure Ni and mild steel. The microstructure of the worn surfaces have been studied and correlated with the wear behaviour.

List of Figures

ii

List of Tables

Chapter 1

Introduction

1.1. Surface Coating

A major challenge in modern engineering material technological development is to meet requirements for new materials for use in progressively more stringent conditions. Usually one or more of a material's properties are incompatible with the conditions prevailing in the operating environment. In the material-environment configuration, the surface of a component is a vital parameter in determining its optimum usefulness. The need for surface stabilization led to the growing demand for coatings and rapid developments in the field of surface engineering.

An example of surface coating can be seen. The evolution of stronger and more creep resistant alloys to enhance thermal efficiency resulted in loss of oxidation and corrosion resistance. Operation of materials at progressively higher temperatures close to the melting points of conventional alloys, where adequate cooling leads to loss of efficiency, has led to the development of ceramic thermal barrier coatings. These coatings enable the attributes of two or more materials (the substrate and the coatings) to be combined to form a composite having characteristics not readily or economically available in a monolithic material. Examples are tribological properties and high strength coupled with corrosion resistance. In the high temperature field, economic and technical pressures to achieve extended lives and greater reliability plus a need to conserve certain relatively scarce (and hence expensive) or strategic alloying elements, have dictated increasing course to coatings.

The outermost surface and the rest of the component can be considered together to form a system. The primary requirement of a protective surface is to have qualities superior to that of the substrate in order to shield the component from an aggressive environment. The system is invariably hybrid, whether it has been achieved by means of a surface modification of the component substrate itself or one or more other materials have been applied as a coating to the component surface. In either case, surface treatment is involved, the choice of which is vast and varied. The combination of coated surface and

substrate is called a coating system and it includes surface modification although it may be more accurate to designate the latter as a surface modified system. Various types of coatings are discussed in the literature review.

1.2. Composite Coatings

Metal matrix composites (MMC) represent an emerging new class of materials as conventional metals and alloys having restricted applications. The purpose of a composite material is to alter and improve the properties of the matrix material, by the addition of some second material with very different chemical and structural properties. Metal-matrix composites are materials in which a metallic host material is modified through the addition of a second phase (ceramic). The second phase may be in the form of particles or fibers. The goal is to supplement the desirable properties of the metal, such as ductility and strength by the addition of a ceramic which can improve the performance of the material in its final application. Common goals in the creation of new metal-matrix composites are to achieve increased strength, reduce friction, or prevent corrosion.

Although metal matrix composite (MMC) materials have been available for the last two decades, they are yet to be tested to their full potential for high temperature behavior and as coating materials [1]. The development of carbon-carbon composites started in 1958 but intense research did not begin until the space shuttle project gathered momentum [2]. The work done by Strife and Sheehan on ceramic coatings for carbon composites was a logical consequence of material modification in the process of optimizing the application of the composite as well as combating its vulnerability to oxidation [3]. Composite coatings and composite/multi-layer coatings have shown a considerable range and potential for development and application in the fields of corrosion, wear, high temperature and space technology [4].

1.3. Wear of Composite Coatings

In general, microhardness, yield strength, tensile strength and wear resistance are all improved by the presence of second phase particles. During the composite electroplating, these fine particles of metallic, non-metallic compounds or polymers are codeposited in the plated layer [5]. The deposition of finely dispersed particles in a metal

2

matrix by electrodeposition processes correspondingly led to a new generation of composites [6].

Keeping in view the demand for different engineering applications of Ni composites with high wear resistance, numbers of investigations are being done on Ni-SiC [6, 7] composites. Using WC as secondary phase can even increases the wear resistance of the composite and there is very little work done in this area as per the author's concern. And investigating the tribological behavior of this Ni-WC composite coated layer by studying the frictional and wear analysis is totally justified.

1.4. Objective

The present study aims at processing and characterizing nickel-tungsten carbide (Ni-WC) composite coatings on mild steel by the electrodeposition technique. The electrodeposition of Ni-WC has been performed using the standard electrolyte solution containing Nickel sulfate $NiSO_4$ $6H_2O$ (250 g/l), Nickel chloride $NiCl_2$ $6H_2O$ (35 g/l), and Boric acid H_3BO_3 (40 g/l) [8].

The project was implemented in two stages. The first-stage involved the familiarization with the basics of composite electrodeposition and optimization of the parameters to obtain optimum composite coatings. In the second stage, experiments were performed with the desired conditions and the corrosion, friction and wear resistance of the composite coating were evaluated. The major variable was the amount of ceramic reinforcement in the coating.

1.5. Plan of Work

The work has been planned to proceed according to the following sequence:

1. Procurement of the chemicals and materials required for elctrodeposition of Ni-WC.
2. Experimental set-up for electrolytic deposition of composite.
3. Preparation of anode and cathode for deposition.
4. Microstructural study of deposited sample.
5. Study of potentiodynamic behavior of the deposited sample in 0.1 mol/liter H_2SO_4 solution.

6. Tribological testing of deposited sample composite.

Chapter 2 deals with the review of the literature. Experimental procedures are discussed in Chapter 3. Chapter 4 presents the results and discussion. Conclusion and suggestions for further work are listed in Chapter 5, followed by bibliography.

Chapter 2

Literature Review

It is well known that electroplating has been developed by empirical methods and that its growth has been largely empirical. In the past, electroplating was limited primarily to fulfilling decorative needs. However, today it is an important industrial process used to confer functional properties such as corrosion resistance, wear and abrasion resistance, tarnish resistance, heat resistance, electrical conductivity, bearing surface and solderability, and also to salvage worn-out components or mismachined parts. In addition, articles can be reproduced (or electrofabricated) by a technique of heavy deposition called electroforming.

Composite material can be described as materials made by the combination of two or more materials and characterized by the properties that the individual components do not have. The main methods for the production of composite material are powder metallurgy, metal spraying, internal oxidation, co-precipitation and electrodeposition. Powder metallurgy is based on mixing of metallic and nonmetallic which are subsequently pressed or extruded and sintered to form products. Such techniques are very attractive due to their lower energy requirements and lower materials losses in comparison with classical casting technology due to no/or limited further mechanical finishing being required after sintering. Metal spraying is based on melting of metallic powders, which are sprayed on the surface of the parts by means of a gas flame, composites being obtained by adding inert particles to the powder blend. By selective internal oxidation of dilute alloys, a very fine dispersion of oxides can be obtained by adjusting the oxidation temperature and alloy composition. Co-precipitation requires easily reducible metal salt and colloidal oxide dispersion. Subsequent reduction of the metal salt produces a mixture of very fine metal oxide powders, which can be further processed by conventional powder techniques. Each of these methods has its own benefits and disadvantages and the choice of a particular technique has to be decided for each specified case.

A new attractive method is electro co-deposition, which allows the production of composites in a coating form, which is especially suitable to the field of tribology (wear, friction and lubrication). Electrodeposition is also being recognized as an effective

technique for the fabrication of composites. Strictly speaking, composite electrodeposition consists of the electrolysis of plating solution in which micron- or sub-micron-size particles are suspended: variable amounts of these particles become embedded in the electrochemically produced solid phase, to which they impart special properties. The work carried out in this field was aimed almost entirely to the production of wear and corrosion-resistant coatings, self-lubricating layers and dispersion-strengthened coatings. The formation of rough deposits was attributed to the presence of impurities in the plating bath and to avoid this, impurities had to be removed by filtration of the bath. This possibility to co-deposit foreign particles is used, but in a controlled way, in order to obtain composite coatings by electrodeposition. The second phase particles are kept in suspension through out the plating period by agitating the bath using different techniques such as mechanical stirring, air agitation, electrolyte circulation, and ultrasonic agitation and fluidized bed methods. New types of agitation techniques called liquid air process and plate pumping process have been suggested by Kedward [9], to effect violent agitation. The particle size of the powder and the type of agitation are important for the process of electro co-deposition. It is possible to deposit almost any particles up to 44 μm. larger size particles are difficult to keep in suspension. Usually particles of size 1 – 3 μm were used to produce smooth deposits. Finer particles usually coagulate and thus prevent uniform dispersion. Particles can also be incorporated in the form of fine fibers.

The variables involved in this process to determine the feasibility of obtaining a dispersed second phase in the deposit are

1. Nature of the matrix metal,
2. Composition of the plating bath and throwing power,
3. pH of the bath,
4. Composition of the nonmetallic phase,
5. Size and shape of the non-metallic particles,
6. Current density,
7. Stirring efficiency (rate of movement of nonmetallic particles).

The relative importance of these variables can be judged from experimental findings. The growing interest in electrodeposited composite coatings is partly due to the flexibility of the process and partly due to the competitive position with respect to other

production techniques (shown in Figure1) for such composite materials. In comparison with alternate methods some advantages for electrodeposited composite coatings can be cited.

- Only a limited financial investment is necessary to adapt a conventional plating cell.

- A wide range of composites can be obtained by selecting different types of inert particles like metal oxides, metal carbides or organic compounds.

- Control of experimental variables permits smooth deposits with dimensions as required, resulting a minimal post plating operations.

- No heating of the parts is required and thus thermal damage of the components to be coated is avoided.

- As compared to metal spraying more complex geometrical forms can be coated successfully.

The principal practical limitations of the electrodeposited composite coatings (ECC) are the grain size of the second phase particles and a limited rate of co-deposition. An ECC consists of a metallic matrix with a dispersion of a second phase, using conventional electrolysis, two types of metallic matrices being possible namely pure metal/an alloy. Every metal/alloy, which can be obtained by electrolysis in principle, can be used as a matrix in an electrodeposited composite coating. Besides the choice of the metallic matrix, consideration has to be given to the choice of second phase which can be a powder or fibers, with further distinction between conducting and non-conducting particles, moreover, fibers can be embedded perpendicular to each other or randomly oriented. A large variety of composite coatings can thus be obtained by electrolysis, and these can be classified into

- Composite coatings with oriented or random fibers structure
- Composite coatings with a metallic matrix and a dispersion of a powder phase
- Composite coatings with a dispersion of a powder phase.

Depending on the type of inert particles chosen, the properties and the applicability of the product may be different; in connection with the choice of second phase there are three limitations:

- The second phase has to be insoluble in the plating bath used.

7
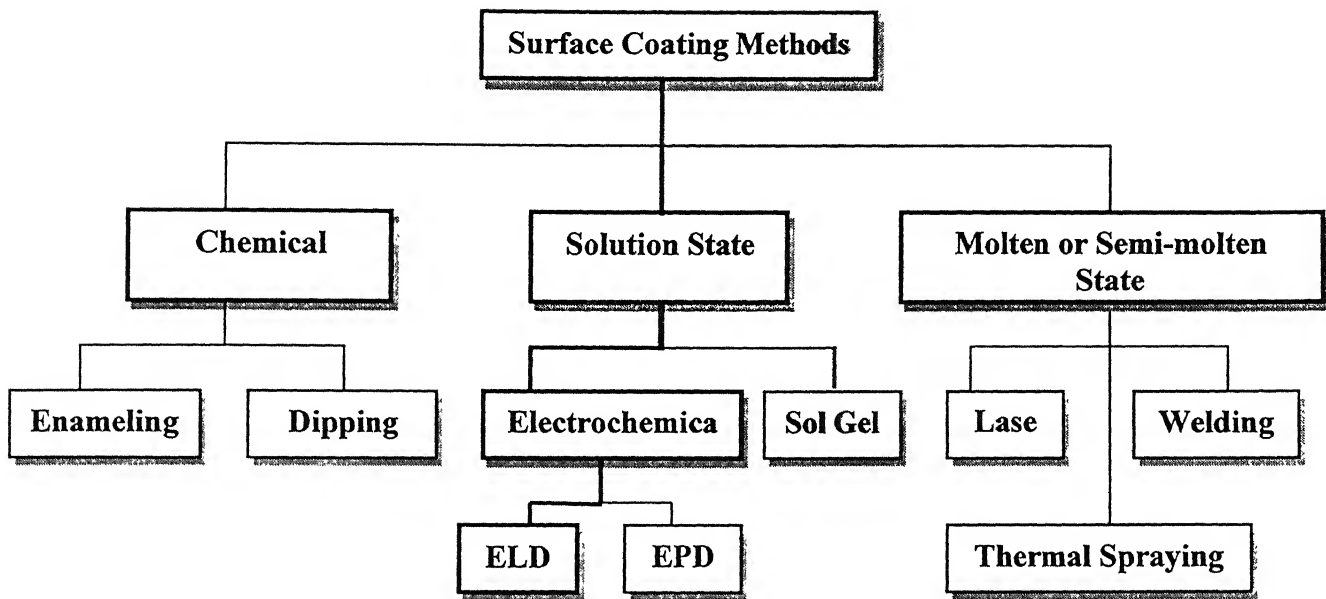
Figure 1 Flow diagram show the various types of surface coating techniques [10].

- It has to be available in powder or fiber form, and
- It has to be wetted by the solution.

2.1. Electrolytic and Electrophoretic Deposition of Composite

The two most prominent ceramic electrodeposition techniques, i.e. electrolytic deposition (ELD) and electrophoretic deposition (EPD), are gaining increasing interest both in academic and in the industrial sector, and a wide range of novel applications in the processing of advanced ceramic materials and ceramic coatings are emerging. The interest in these processes is based not only on their high versatility to be used with different materials and combinations of materials but also because these are cost-effective techniques usually requiring simple equipment. Moreover they have a high potential for scaling up to large product volumes and variety of product shapes.

ELD leads to thin ceramic films from solutions of metal salts by production of colloidal particles in electrode reactions. Thus, electrode reactions in ELD and electrophoretic motion of charged particles in EPD result in the accumulation of ceramic particles and formation of ceramic films at the relevant electrodes.

EPD is achieved via motion of charged particles dispersed in a liquid towards an electrode under an applied electric field. Deposit formation on the electrode is achieved via particle coagulation.

2.1.1. Electrolytic deposition (ELD)

Electrolytic deposition produces thin ceramic films from solutions of metal salts and it is a relatively new technique in ceramic processing. There are several basic mechanisms of ELD of ceramic films. Cathodic electrolytic deposition has important advantages and can be used for deposition of various oxide materials. In the cathodic electrodeposition method, cathodic reactions are used to generate OH^- groups and increase the pH at the electrode. Metal ions or complexes, which are stable in the bulk of solutions

at low pH, are hydrolyzed by electrogenerated base at the electrode surface to form colloidal particles. These particles coagulate to form cathodic ceramic deposits.

Several studies have recently contributed to both the fundamental understanding of the mechanisms of ELD and the practical use of ELD for various applications. The most significant advances are summarized in this section.

2.1.1.1. Fundamental principles of the ELD process

Mechanism of cathodic electrodeposition has come from the application of the classical DLVO theory of colloidal stability. Electrolyte concentration in the solutions used for ELD exceeds the flocculation values for corresponding ions. Therefore colloidal particles obtained by cathodic electrosynthesis are unstable and coagulate to form a cathodic deposit. The important recent finding is that the formation of a ceramic deposit during ELD is caused by flocculation introduced by the electrolyte [11]. In a recent review by Zhitomirsky [12], chemical strategies and developments of cathodic electrodeposition, focusing on the fundamentals and principles of the process, have been covered.

2.1.1.2 Coatings for electronic, catalytic and optical applications

Electrolytic deposition has aroused considerable interest for the development of thin films of Titania and complex titanates for applications in electronics. What is very important about this recent work is that a relatively low temperature is required for film crystallization, i.e. the formation of a perovskite phase was observed at 500^0C.

Ishikawa and Matsumoto [13], used alternative electrolysis in $(NH_4)_2[TiO(C_2O_4)_2]$ solutions for electrodeposition of TiO_2 into porous substrates. The deposits showed high photocatalytic activity for the decomposition of acetaldehyde. Another important approach is based on anodic oxidative hydrolysis of $TiCl_3$. This method was applied recently to produce TiO_2 nanowires [14]. Well-aligned TiO_2 nanowire arrays prepared by this method could be useful for photoelectrochemical applications.

Pauporte and Lincot [15] reported epitaxial growth of zinc oxide films on single crystal GaN layers. Prepared films exhibited good optical and luminescence properties. The important finding was the possibility of tuning of film properties by changing the applied potential, bath composition or by post-deposition thermal treatments. Particular importance. is the recently demonstrated possibility of epitaxial deposition of ZnO nanopillars onto Au (111), Au (110) and Au (100) single crystal substrates [16]. It was suggested that these nanopillars could be used as templates for molecular electronics and for data storage.

A promising ELD approach has been exploited for preparation of macroporous ZnO films [17]. In this method highly ordered macroporous ZnO films were electrodeposited using polystyrene colloidal crystals as templates. These results have the way for formation of advanced films combining photonic, luminescent and piezoelectric properties. Similar strategies might be used for a number of other photonic crystals.

2.1.1.3. High-temperature coatings and solid oxide fuel cells

Important developments were reported in the field of electrodeposition of materials for high temperature applications. Advanced ceramic coatings were deposited for protection of stainless steel against oxidation at high temperatures [18]. It was demonstrated that protective properties of ceramic coatings could be improved by the use of additives.

The interest in ELD for fuel cell applications stems from the need to decrease the thickness of the electrolyte layer and deposit intermediate layers preventing interfacial electrode-electrolyte degradation at elevated temperatures. Thin films of yttria-stabilized zirconia and $Ce_{1-x}Gd_xO_{2-y}$ were prepared by cathodic electrolytic deposition [19]. It was shown that the critical thickness of electrolytic deposits achievable without crack formation could be increased using a cationic polyelectrolyte with inherent binding properties.

2.1.1.4. Biomedical applications

Considerable attention has been given to electrodeposition of ceramic coatings for biomedical applications. The interest in electrolytic deposition for implant development stems from the possibility of deposition on substrates of complex shape and the high purity of the deposits. Dinamani and Kamath [20] prepared various phosphate materials using cathodic electrodeposition. Manso *et al.* [21] reported electrodeposition of hydroxyapatite coatings in basic conditions. These hydroxyapatite coatings exhibited good adhesion to the substrates.

The problem of cracking in electrolytic zirconia deposits, which usually occurs upon drying, has recently been addressed by the use of polymer additives [22]. It was shown that (polydiallyldimethylammonium chloride) (PDDA) act as a binder, providing better adhesion of zirconia deposits and preventing cracking. An important finding was that the amount of organic phase in the deposits could be changed by variation of PDDA concentration in solutions. These results have the way for ELD of thick hybrid bioactive organic and inorganic films.

2.1.2. Electrophoretic deposition (EPD)

The phenomenon of electrophoresis has been known since the beginning of the 19th century and it has found application in the past 40 years mainly in traditional ceramic technology. EPD is essentially a two-step process. In the first step, charged particles suspended in a liquid migrate towards an electrode under the effect of an electric field (electrophoresis). In the second step, the particles deposit on the electrode forming a relatively dense and homogeneous compact or film. A post-EPD processing step is usually required, which includes a suitable heat-treatment (firing or sintering), further densify the deposits and to eliminate porosity.

In general, EPD can be applied to any solid that is available in the form of a fine powder (<30 μm) or a colloidal suspension. Indeed, examples of EPD of any material class can be found, including metals, polymers, carbides, oxides, nitrides and glasses [23, 24].

The potential of the EPD technique for the realization of unique microstructures and novel (and complex) materials combinations in a variety of shapes and dimensions is being increasingly appreciated by materials scientists and technologists.

2.1.2.1. Fundamental principles of the EPD process

The basic mechanisms of EPD shown in Figure 2 have been extensively considered in the literature mainly in the framework of the Derjaguin-Landau-Verwey-Overbeek [24] (DLVO) theory and particle double layer distortion on application of D.C., electric field. There are however multiple theories put forward to explain particle interactions and kinetics of deposition and further theoretical and modeling work is being carried out. Numerical simulation has been used for the first time recently to model the buildup of a deposit of charged particles on an electrode during EPD [25, 26]. These studies are both of fundamental and practical interest as they provide insight into local variations of particle interaction processes during deposition, which can be used, for optimization of EPD techniques Sarkar *et al.* [27] have provided important fundamental study on the formation of colloidal films during EPD. They observed the deposition of silica particles on silicon wafers as a function of deposition time, and compared the nucleation and growth of the silica particle layer with that of atomic film growth via molecular-beam epitaxy. A striking similarity was found between the two growth processes. This indicates possible new directions for further research as the equivalence between the two processes provided insight into the growth kinetics of EPD films and can be used for their microstructural optimization.

2.2. Composite Coatings

Electrodeposited composite coatings are produced by suspending the second-phase materials, in the form of fine powder or filaments, in a conventional plating electrolyte. These particles are held in suspension throughout the plating period by agitation.
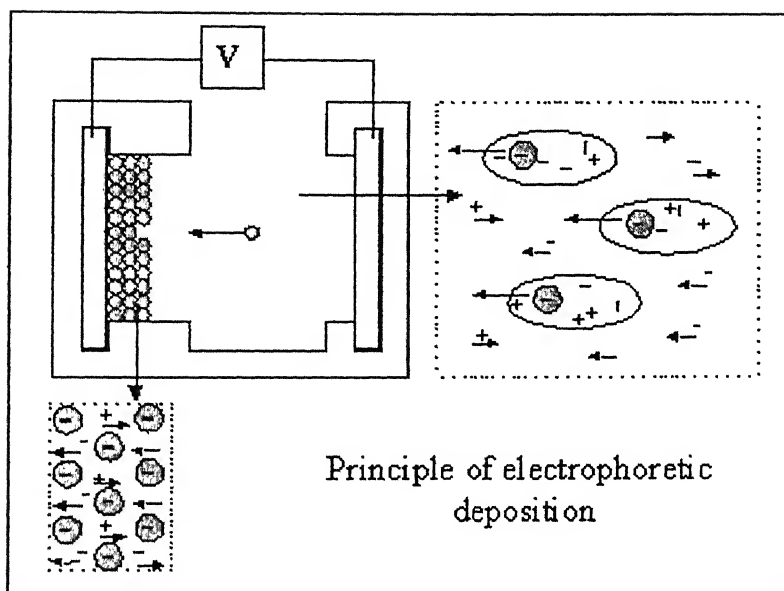
Figure 2 Schematic of cathodic electrophoretic deposition (EPD), showing electrophoretic motion of charged ceramic particles [24].

Depending upon the intended application, composite could be categorized into the following:

2.2.1. Wear resistant coatings.

2.2.2. Dry lubricant coatings.

2.2.3. Oxidation and Corrosion resistance coatings.

2.2.4. Heat treatable metal alloy coatings.

2.2.5. Nuclear control coatings.

2.2.1. Wear Resistant Coatings

These are formed by codepsition of refractory powders like SiC, Al_2O_3, WC, ZrB_2, TiO_2 etc. Most of the workers have tried to develop this type of elecrodeposited composite coatings. The wear resistance and erosion resistances are thought to be developed for the following reasons.

When a composite coating having hard dispersed particles is brought into contact with a sliding counterface the wear continues till the hard particles are exposed so that they bear the wear load. However, Kedward [9] pointed out that in actual practice a certain amount of metal to metal contact was inevitable due to non-uniformity of the applied load over the wearing surface. Accordingly it can be presumed that maximum wear resistance would be obtained when the hard particles were dispersed in a hard and wear resistant matrix, also a material is expected to possess good wear resistance when it has low mutual solubility and low surface energy to hardness ratio. With these assumptions many investigators tried to codeposit hard particles like Al_2O_3, TiO_2, SiC, WC, Cr_3C_2, TiC, diamond etc. in the range of metal matrix such as Ni, Cr, Co, Re, etc.

It was found that in Ni matrix most of the fine oxide particles could be codeposited easily using the conventional Watts/sulphomate bath. Ramanaskene [28] successfully codeposited particles of SiO_2, Al_2O_3 with Ni from Watts-type solutions. However, the concentration of solid particles in the Nickel deposit was low up to 1 Wt% SiO_2 and up to 4 wt. % Al_2O_3. Malone [29] studied the Ni-thorium oxide in both the sulphomate and watts type electrolyte and showed that electrodeposition can be successfully employed to produce dispersion-strengthened materials.

Ristic and Pavicevic [30] investigated the bond between Al and Ni in Ni-Al_2O_3 system and found that it can be either ionic-covalent or metallic one. The electronic structure of the inter-atomic bond was very similar to Ni_2Al_3 alloy type but was not identical with it. The complex structure of Kβ band consisting of Al 3s, 3p levels and Ni 3d, 4s levels which could be better interpreted by the application of MO theory. The properties and structure of SKα lines resulted from redistribution of electronic charge and strong interaction of Al 2p levels and Ni 3p levels. This will be useful in understanding the fundamental aspects of the structure of the composite coating system, which in turn will be helpful in predicting the bond strength of the second phase particles with the metal matrix. Sayfullin *et al.* [31] produced Ni composite coatings at non-stationary parameters of electrolysis. They found that the cleanliness of composite electro-chemical coatings (CEC) and the uniformity of the second phase distribution increased with the increasing amplitude of anode. The use of non-stationary electrolysis enabled the range of CEC physical properties to be widened. Suchentiunk [32] produced dense, homogeneous and pore-free composites by embedding high strength fibers like boron carbide coated boron fibers in electrodeposited metals (Cu, Ni, Al). This technology was utilized in producing pressure vessels for space applications Sayfullin *et al.* [33] were able to produce Al-alumina coatings of any thickness from a bath containing equal parts of $AlCl_3$ and $LiAlH_4$ in tetrahydrofuran solutions plus dispersed corundum particles. They found that the microhardness of the coating could be as high as 1310 Mpa for a coating containing 19 % alumina. Also they found that the cathode and anode yields of Al were approximately 100 %. Their deposition rate was 12 μm per hour at a current density of 1 amp/dm^2.

Compared to Ni, hard matrix of Cr was found to be much more attractive due to its good wear and oxidation properties. Unfortunately the chromium plating process possesses very poor cathode efficiency and microthrowing power.

Composite coating using copper as matrix metal have been produced from sulphate and alkaline cyanide bath. Unlike Nickel, Copper gave great difficulty in codeposition. Using copper cyanide solution silica, alumina, and silicon carbide could all be deposited with copper very easily. But conducting particles like W, Cr is codeposited more readily from acid solution. Like Nickel cermets, copper cermets are also capable of withstanding high temperature operation. Cu-Al_2O_3 composite with 6.5 % of Al_2O_3 by volume was

reported to be unaffected even after annealing at 800^0F and hardness and tensile strength was twice that of pure copper deposit after heat treatment. Snaith and Grooves [35] studied the codepositon process of silicon carbide, quartz and chromium diboride with copper from conventional $CuSO_4$ bath where zeta potentials and surface charge density played an important role in their process of code position. But Malone [30] failed to yield a composite of copper and gamma alumina form conventional acid copper electrolyte bath by using and not using promoters as described by Tomaszewski [36].

Cobalt (hcp structure) possesses good wear and frictional characteristics. So production of cobalt borides has found many commercial applications. However, due to its relatively low bulk hardness (400 Vpn as deposited) their uses for combating abrasive wear are limited.

Only a few researchers endeavored codepositing second phase particles in the alloy matrix and not many papers are available in the literature, in this area. Most of the works are done either by Japanese or Russians, all the journals are in their own languages. Their English translations are scarcely available.

Devernikova et al. [37] successfully codeposited boron particles in the Ni-P matrix. They found that the boron particles had a marked effect on the phosphorous content of such coatings and the rate of deposition of Ni. Diffusion annealing of Ni-P-B coatings lead to the formation of a new phase and an improvement in their physio-mechanical properties, in particular hardness and wear resistance.

Saifullin et al. [38] studied the role of fine α alumina ZrO_2, TiO_2, graphite and MoS_2 particles on the mechanism of electrodeposition of Ni-P and Co-P on the metal substrate. They found that with increasing concentrations of alumina and graphite in the electrolytes the current yields of Co-P alloy increased. Cathodic polarization curves showed that increased graphite particles concentrations activated the cathodic surface, whereas Al_2O_3 particles shifted the cathodic potential to the electro negative region, i.e. they hindered cathodic process. Toshiba corporation of Japan registered [39] a patent for the wear resistant coating in which they co-deposited $Fe_{80}B_{20}$ particles with the Ni-P electrodeposit using a plating bath containing nickel sulphomate, nickel chloride, H_3BO_3, sodium saccharin, phosphorous acid and $Fe_{80}B_{20}$ particles. Krivoshchepov et al. [39] studied the structural transformations of dispersed systems in an electric field. They found

17

that Al^{3+}, Al (OH) $^{2+}$ and Al (OH) $_2^+$ ions were present in the Al_2O_3-H_2O systems when the pH was greater than 8. Also they found the maximum dependence of the zeta potential on pH is at pH $1.5 - 2$ and $9 - 9.5$. The zeta potential and viscosity changes were not affected by particle size. Suspensions with a particle size 4μm were more stable than those with particle size 40μm and could be used for preparation of ceramic coatings by electrodepositon. Ni coating containing $2 - 10$ wt% of P in which silicon nitride particles dispersed was coated on the sliding parts of steel and they were subsequently surface hardened by heat treatment. The parts had excellent abrasion resistance as piston rings in an engine test.

2.2.2. Dry lubricant coatings

It is expected that if some soft particles having low shear strength were dispersed in a metal matrix then the resulting composite coating would possess good antifriction properties. So various lamellar lubricant phases (e.g.) MoS_2, graphite, $BaSO_4$ were tried to codeposit with Ni, Cr, Cu, Ag, Sn etc. Codeposition of lamellar solids proved to be much more difficult to achieve than codeposition of ceramics. Some investigators tried to replace it by resinous material such as P.T.F.E., Polyolifine, plyphenylene, pvc plymer etc. Most extensive studies have been made in the codeposition of $BaSo_4$ in Ni (or Cu since they are useful in sliding contacts due to antistick proposition of $BaSO_4$ with Cu in acid $CuSO_4$ bath required specific additives.

2.2.3. Corrosion and oxidation-resistant coatings

A well-known application of codepsition to improve the corrosion resistance of coatings is the production of microporous chromium layers by codepositon of non-conducting particles in the underlying Ni layer. Corrosion of the Nickel will thus occur over an increased surface resulting in a smaller depth of attack. Other examples are Cr-ZrC coatings, which offer good resistance to sulphur corrosion. In an oxygen-enriched atmosphere Ni-Al_2O_3 composite coatings have better oxidation-resistance than plain nickel and good results are also reported for elecrodeposited nickel silicon carbide composites by Stoott and Ashby [41]. The introduction of fine silicon carbide particles causes a significant decrease in oxidation rate, largely due to internal oxide derived particles acting

as barriers to Ni^{3+} diffusion through the NiO scale. A recent report on the oxidation behavior of Cobalt-Chromium carbide electrodeposits [42] confirms that the moment of oxygen through oxidation scales is a significant factor in the oxidation characteristics of these composites. It was shown that first carrying out an inert atmosphere heat treatment to produce homogeneous alloy could, significantly increase the oxidation resistance of electrodeposited cobalt-Chromium carbide composite coatings. Due to the complexity of corrosion and oxidation environments it is difficult at present to give a rational explanation of these various observations and performance tests are required for each new application.

2.2.4. Heat treatable metal alloy coatings

Recently the most interesting area of ECC development is that of producing heat treatable coatings and electroforms. Bazzard and Boden [43] have shown that Cr powder can be codeposited with Ni and heat-treated to produce Ni-Cr alloy. By this technique copro-Nickel, Stellite, ball bearing steels have been produced. Metal powders and ceramics codeposited simultaneously with Cr and Co-Mo alloy are being developed as high temperature corrosion and oxidation, resistant coatings. Also Sayfulline has successfully produced Cu-Ag alloy having a high hardness with 8 –14% inclusion of Ag powder [44]. Codeposition of Ni powder in Ni matrix in electron tubes has been studied by varadi et al. Such a Ni matrix improves heat and electrical conductivity and minimizes the detrimental effect of high voltage sparking. Cahassaing *et al.* [45] investigated the Ni-Mo and Co-Mo electrodeposits as a function of molybdate concentration in a citrate complex bath.

2.3. Mechanism of Composite Electrodeposition

Different investigators have proposed different possible mechanisms, which are mechanical entrapment, electrophoresis, and two-stage adsorption mechanism. These mechanisms will be described in detail below.

2.3.1. Mechanical entrapment

The mechanical entrapment can be described as a probability process in which the particles are brought in to contact the electrode by agitation of the plating bath. So if the metal deposition is sufficiently high, the particles, which will be delayed at the cathode,

19

will be trapped by the flux of the depositing metal and eventually engulfed in the deposit. Hence the cathode is important for obtaining co-deposition by this mechanism. But during violent agitation of electrolyte, it is quite improbable for a particle to be attached to the cathode surface, during which metal matrix would grow around to make it stable. Brands and Goldthorpe [46] showed that Al_2O_3 can be deposited with Ni-acid bath but not with Cu-acid bath though the cathodic efficiency of copper is 95 %. They concluded that the particle entrapment depended upon micro-throwing power and not on the metal deposition rate. Electrolyte with good micro-throwing power would be expected to plate behind the particles and move it away from the cathode along with the growing metal, while one with poor micro-throwing power would be expected to build up around and entrap the particles. Moreover, large particles, due to its higher gravitational force, promote downward moment i.e., the cube of particle radius and the attractive force due to surface charge, which could be proportional to the square of radius vary differently depending up on the particle size. Therefore, ideas was directed towards the importance of surface charge of particle, which can describe the codeposition process more clearly.

2.3.2. Electrophoresis

Electrophoresis is a phenomena by which charged particle, placed in a liquid, moves under the influence of an applied electric field. The nature of the surface charge will decide the direction of the particle movement. Positively charged particles will move towards the cathode and negatively charged particles will move towards anode. The velocity of moving particles can be given as

$$V = \frac{DE\,\zeta}{4\pi\mu} \qquad (1)$$

where V = electrophoretic velocity, E = applied potential gradient, D = dielectric constant of medium, ζ = zeta potential, μ = coefficient of viscosity of the medium, for particles possessing a zeta potential of +20 mV, moving under the potential gradient of 0.25 V/cm. The electrophoretic velocity calculated from the above expression is 5×10^{-5} cm/s. The hydrodynamic transport by agitation is of the order of 5 cm/s, which is very high compared to electrophoretic velocity. However, once a particle reaches the electrical double layer of

the cathode, the electrophoretic transport becomes important, because the hydrodynamic transport of particles would be generally parallel to the cathode surface. The voltage drop across the double layer is much higher than in the bulk of the medium because it occurs over a relatively small distance (100-500 μm) and may be sufficient to cause electrophoretic transport of the particle to the cathode.

2.3.2.1. Electrokinetic phenomena

The movement of charged colloidal particles in electric field is termed electrophoresis. When the charged solid surface is fixed, the electric field causes a movement of the liquid called electroosmosis. Forcing a liquid through a capillary or porous plug induces a difference of electric potentials called streaming potential. Forced movement of charged solid particles in a liquid, e.g., due to gravitation induces a difference of electric potentials, the sedimentation potential.

The velocity in electrophoresis and the difference of pressures between two ends of capillary or porous plug in electroosmosis is proportional to the applied field strength. The streaming potential is proportional to the applied pressure. The sedimentation potential is proportional to the velocity of the particles. The electrokinetic's phenomena often accompany one another; e.g., electrophoresis is always accompanied by electroosmosis due to electric charge of the wall of electrophoretic cell.

2.3.2.2. Zeta potential

The shear plane (slipping plane) is an imaginary surface separating the thin layer of liquid bound to the solid surface and showing elastic behavior from the rest of liquid showing normal viscous behavior. The electric potential at the shear plane is called zeta potential. In the first, rough approximation, the electrophoretic mobility (the ratio of the velocity of particles to the field strength), induced pressure difference in electroosmosis, streaming potential and sedimentation potential are proportional to the zeta potential. The stability of hydrophobic colloids depends on the zeta potential: when the absolute value of zeta potential is above 50 mV the dispersions are very stable due to mutual electrostatic repulsion and when the zeta potential is close to zero the coagulation (formation of larger assemblies of particles) is very fast and this causes a fast sedimentation. Even when the

surface charge density is very high but the zeta potential is low, the colloids are unstable. Also the velocity of heterocoagulation (coagulation of different particles) depends on the zeta potentials of both kinds of particles. Therefore, the zeta potential is an important parameter characterizing colloidal dispersion.

2.3.2.3. Smoluchowski equation

In the past, electroosmosis was the most popular method to determine the zeta potential. Nowadays, electrophoresis has the greatest practical meaning and many commercial fully automatic instruments are available. Marian Smoluchowski was the first who has properly derived an equation to calculate the zeta potential from electrokinetic mobility:

$$\mu = \frac{\zeta \varepsilon}{\eta} \qquad (2)$$

where μ is the electrophoretic mobility, ε is the electric permittivity of the liquid and η is the viscosity.

The measurement of zeta potential helps to explain the difficulty of co-deposition of some particles in certain bath and also the effect of addition of promoter in the bath. The electrodeposition of Al_2O_3 by Sykes and Alner [47] on watts Ni-bath and acid copper bath found that the zeta potential is negative so they concluded that the electrophoretic transport of particles would not take place in this bath.

2.3.3. Two-stage adsorption mechanism

The electrophoretic effect could explain the observed dependence on current density but some difficulty would arise as far as the nonlinear concentration is concerned. Gulielmi [48] proposed a different mechanism based on two successive adsorption steps. In the first step of this mechanism the particles are said to be loosely adsorbed ions and solvent molecules break away from the particles so that a strong and irreversible electrochemical adsorption of particles on the cathode takes place. Then these particles are

engulfed in the depositing metal. With a few elementary hypotheses about the mechanism that governs the two steps, a general expression relating the concentration of the embedded particles to its concentration in suspension and electrode over potential can be written as an equation.

$$\frac{C}{\alpha} = \frac{Wi_0}{nFdV_0} \times e^{(A-B)\eta} \left(\frac{1}{K} + C\right)$$

(3)

where, C= concentration of particles in the bath (vol %), α = concentration of the particles in the deposit layer (vol%), W = atomic weight of the deposited metal, n = valence of the metal, d = density of the metal, F= Faraday constant, η = overpotential, K = adsorption constant, i_0, A = constant related with metal deposition, and V_0, B = constant related with particle deposition

At different values of over potential η. if C/α plotted against C, we obtain a set of converging at the point where C=1/K. Codeopsited particles (α) would increase with increase in current density and if B<A i.e., the slope of the straight line is positive, the volume fraction of the codeposited particles (α) would decrease in current density. This mathematical formulation gives an idea about the kinetics of codeposition process and subsequently the rate-controlling step (slowest step) also can be determined.

Based on results of streaming potential and adsorption studies on alumina in nickel and copper electrolytes it was shown that the nature of the acquired surface charge of the alumina was an important factor in its ability to be codeposited. From their results, Foster and Kariapper [49] concluded that the codeposition occurs in nickel plating baths due to strong adsorption of nickel ions on the particle surface, codeposition of γ – alumina does not occur in acid copper plating baths because cation adsorption on the particle surface is very small, but addition of thallium and rubidium ions to the acid copper bath produces a large positive charge on the alumina surface, there by promoting codeposition. The validity of the model proposed by Guglielmi for the codeposition of alumina and copper from an acidified copper sulphate plating bath was shown in 1977 by Celis and Roos [50]. From

their results on the codeposition in copper plating baths with and without the addition of monovalent thallium ions, they concluded that the second adsorption step is the rate determining. In that adsorption step real contact between particle and cathode is created once anion adsorbed on the particle is reduced at the cathode surface and they showed that only when the reduction of the copper ions is under charge transfer over voltage control a considerable increase of the amount of embedded alumina particles is obtained with increasing current densities, when the concentration over voltage becomes predominant the amount of codeposited particles decreases with increasing current densities. Once the applied cathode over voltage is large enough to reduce other ions adsorbed into particles as e.g. hydrogen ions, higher codeposition is obtained.

2.4. Parameters Influencing Coating

Various parameters that influence deposited material and properties, which are concentration of the bath, particle size, current density, temperature, time of deposition, bath load, and surfactants.

Prabhakaran [50] studied the effect of WC content in the Cr-WC coating and cathode current efficiency. He observed that by increasing current density and bath load, weight of the WC particle in the composite was increased.

Rajnarayan and Chattopadhyay [51] studied the coating of Cr-Al$_2$O$_3$ composite on mild steel. Initially they attempted to codeposit as-received Al$_2$O$_3$ with chromium from a conventional hexavalent bath. However, variation in the particle size of the Al$_2$O$_3$ content in the bath and the current density could not produce any composite coating. Foster and Kariapper [48] showed that the concentration of nickel ions in the bath affects the codeposition of Ni-Al$_2$O$_3$ composite coatings. Changing the Cr$_2$O$_3$ concentration, however, did not produce any Cr-Al$_2$O$_3$ composite coatings.

From above experiments it is evident that codeposition of, as received Al$_2$O$_3$ with chromium from the conventional hexavalent chromium bath is not possible. The surface properties of Al$_2$O$_3$ had to be altered before it could be codeposited with chromium. Young [52] showed that codeposition of diamond particles with chromium became possible only when they were covered with a nickel coating. Al$_2$O$_3$ particles were therefore, coated with nickel using an electroless nickel-plating bath. The amount of Al$_2$O$_3$ in the composite

coating increased with increasing Al_2O_3 content in the bath shown in Figure 3. Variation in the Al_2O_3 content in the plating bath showed that at 20A/dm^2, codeposition took place only when the Al_2O_3 content in the bath was more than 60 g/l; beyond this value its amount in the composite coating increased with increasing the bath load of Al_2O_3. Similar behaviour was observed at higher current densities except that codeposition started at much lower bath loads as shown in Figure 4.

Variation in the bath temperature at 30 A/dm^2 and different bath loads showed that heavily cracked deposits were formed at temperatures below 40^{0}C. At higher temperatures an increase in the temperature decrease the amount of Al_2O_3 codeposited at bath loads lower than 60 g/l. At higher bath loads, increasing the temperature beyond 50^{0}C had almost no effect. The thickness variation of the composite coating was of the same order that of the chromium coating as shown in Figure 5. The microhardness of the Cr-Al_2O_3 composite coatings was always higher than that of a pure chromium coating deposited under the same plating conditions as shown in Figure 6(a). At a given current density the microhardness of the composite coating increased with increase in Al_2O_3 content either in the bath or in the coating. Figure 6(b). At a given bath load, the microhardness of the composite coating increased with decreasing bath temperature and increasing current density as shown in Figure 7.

2.5. Electrochemical Corrosion

Corrosion can be defined as the degradation of a metal by an electrochemical reaction with its environment [53]. All metals are found in their low energy state ores, in the form of their oxides, sulfides, carbonates or more complex compounds. Large amount of energy is supplied in order to extract a pure metal from its ore. This pure metal is a high-energy state of the metal and hence they try to come back to the low energy state by recombining with the environment. This process is called corrosion. Figure 8 shows the thermodynamic energy profile for metals and their compounds. The thermodynamic aspects of corrosion will be briefly discussed. All the interactions between elements and compounds are governed by the free energy changes (ΔG). Any reaction is said to be spontaneous when ΔG for the reaction is negative. At room temperature most of the
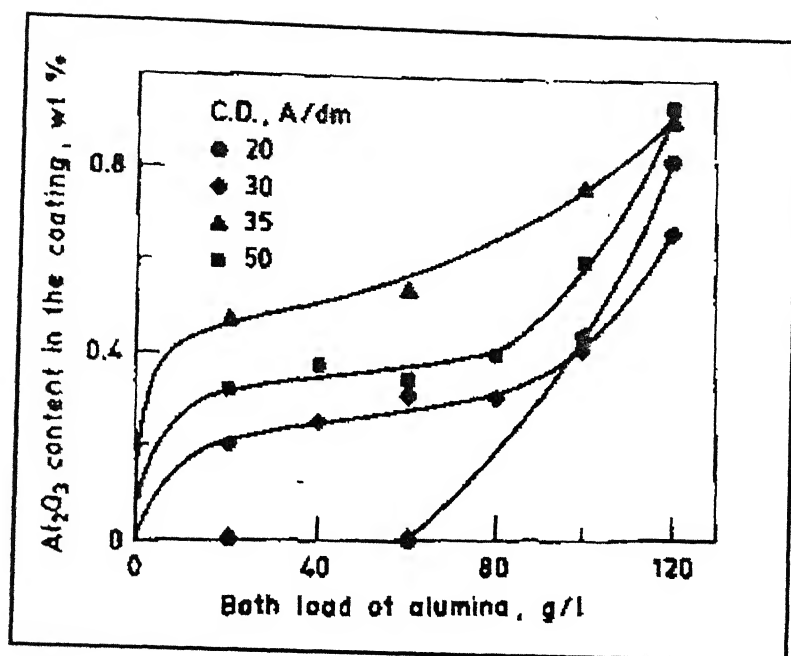
Figure 3 Effect of bath load of Al_2O_3 on its content in the coating at 50 ^{0}C [51].
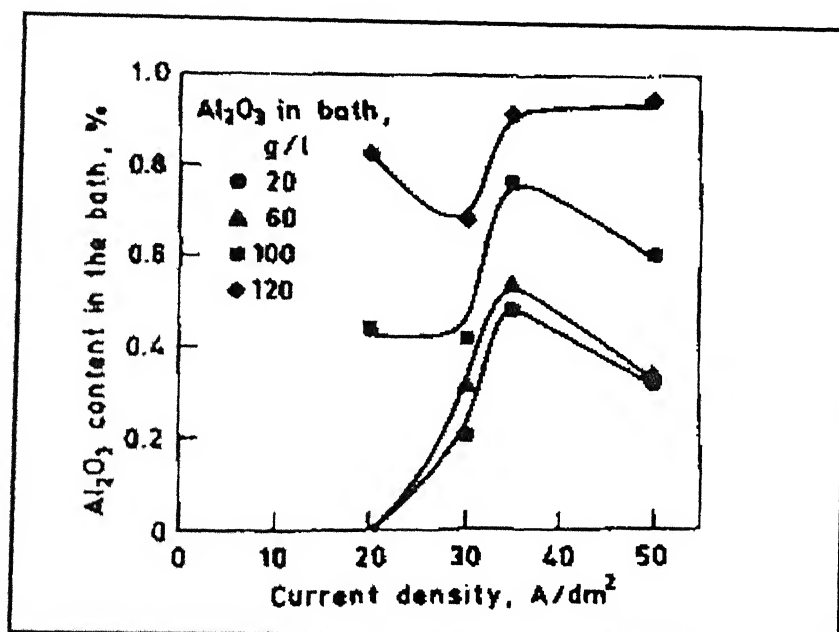
Figure 4 Effect of current density on the Al_2O_3 content in Cr- Al_2O_3 composite coatings at different bath loads [51].

26
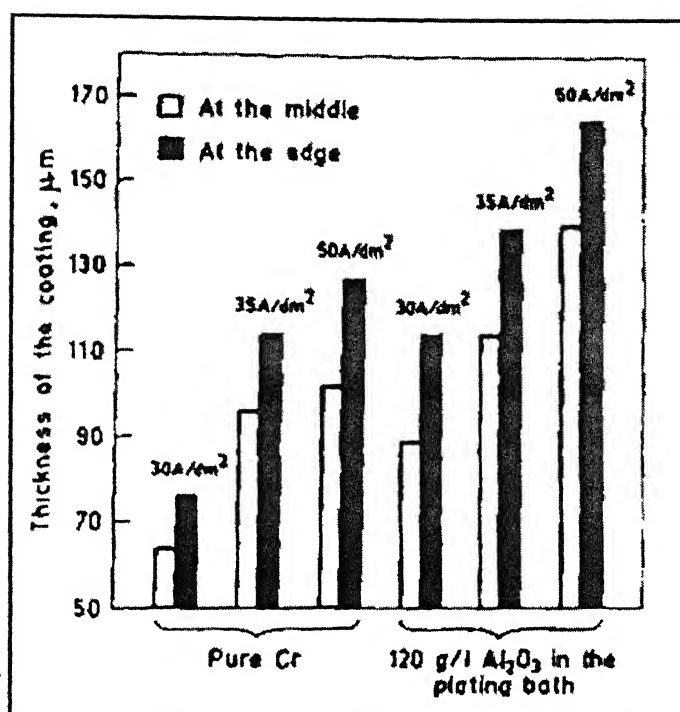
Figure 5 Variation in thickness of the pure chromium and Cr- Al₂O₃ composite coatings deposited at different current densities [51].
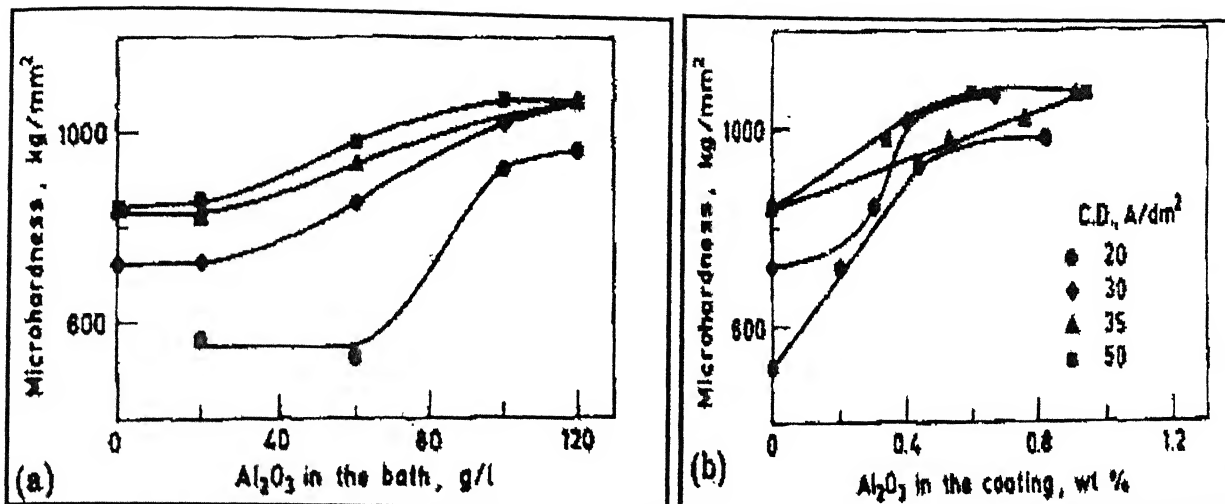
Figure 6 Variation in the microhardness of the coating with Al_2O_3 content in (a) the bath and (b) the coating at 50 ^{0}C [51].
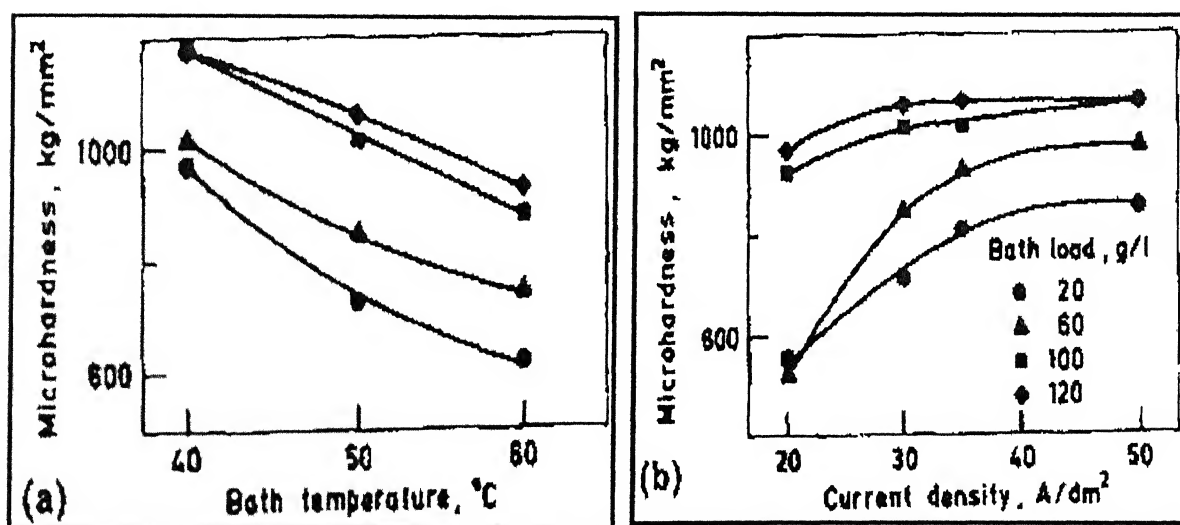
Figure 7 Shows the variation in micro-hardness with a) bath temperature and b) current density [51].

chemical compounds of metals have lower free energy than the pure metals and hence most of the metals have an inherent tendency to corrode.

In all kinds of aqueous corrosion, there are two reactions occurring at the metal/liquid interface; an electron producing reaction (anodic or oxidation reaction) and an electron consuming reaction (cathodic or reduction reaction). The corrosion reaction for the creation of a wet electrochemical cell requires four basic requirements, the cathode on which the reduction reaction occurs, an anode on which oxidation occurs, an electrolyte to act as the conducting medium for ions and a electrical connection for electron to flow between the anode and cathode. The anodic reaction is invariably corrosion of the metal as shown in equation 4. Several cathodic reactions can occur during corrosion [54]. The simplest of them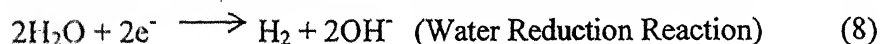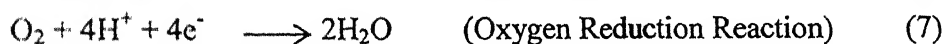 is reduction of hydrogen ions (equation 5). Another is reduction of an oxidized ion in solution (redox reaction) as in equation 6. Another reaction is reduction of dissolved oxygen as in equation 7. In the absence of any of these reactions water reduction will occur as in equation 8.

$$M \longrightarrow M^{n+} + ne^- \qquad \text{(Anodic Reaction)} \qquad (4)$$

$$2H^+ + 2e^- \longrightarrow H_2 \qquad \text{(Hydrogen Reduction Reaction)} \qquad (5)$$

$$Fe^{3+} + e^- \longrightarrow Fe^2 \qquad \text{(Redox Reaction)} \qquad (6)$$

$$O_2 + 4H^+ + 4e^- \longrightarrow 2H_2O \qquad \text{(Oxygen Reduction Reaction)} \qquad (7)$$

$$2H_2O + 2e^- \longrightarrow H_2 + 2OH^- \quad \text{(Water Reduction Reaction)} \qquad (8)$$

A basic wet corrosion cell is shown in the Figure 9. The potential difference between the anode and the cathode could be measured by using a voltmeter in the circuit. But this gives only the potential difference between the electrodes and inorder to measure the absolute potential we need a third electrode. This third electrode is called as the standard electrode against which all the measurements can be made. The standard hydrogen electrode, saturated calomel electrode (SCE) etc, is usually used as the standard electrodes. The Table 1 gives some commonly used standard electrodes and their potentials.
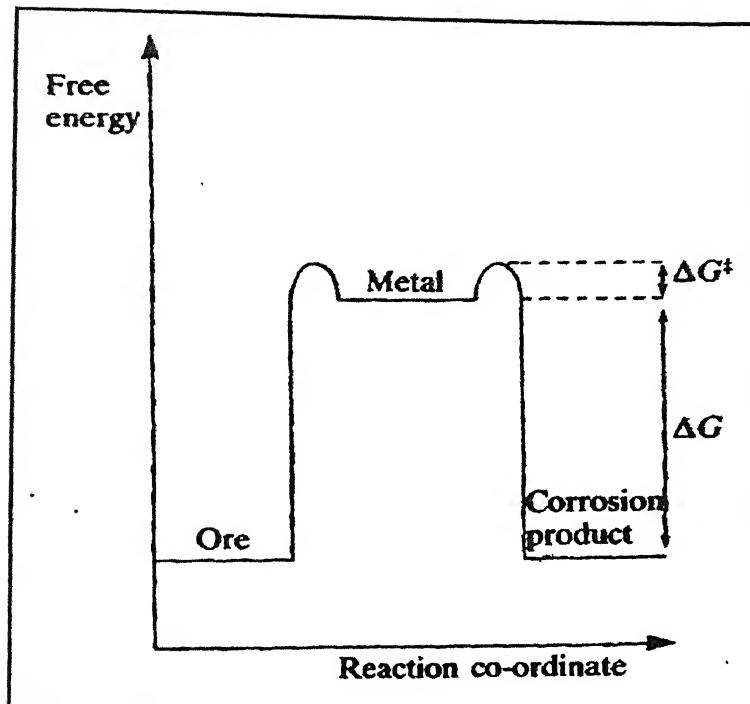
Figure 8 Thermodynamic energy profiles for metals and their compounds [53].
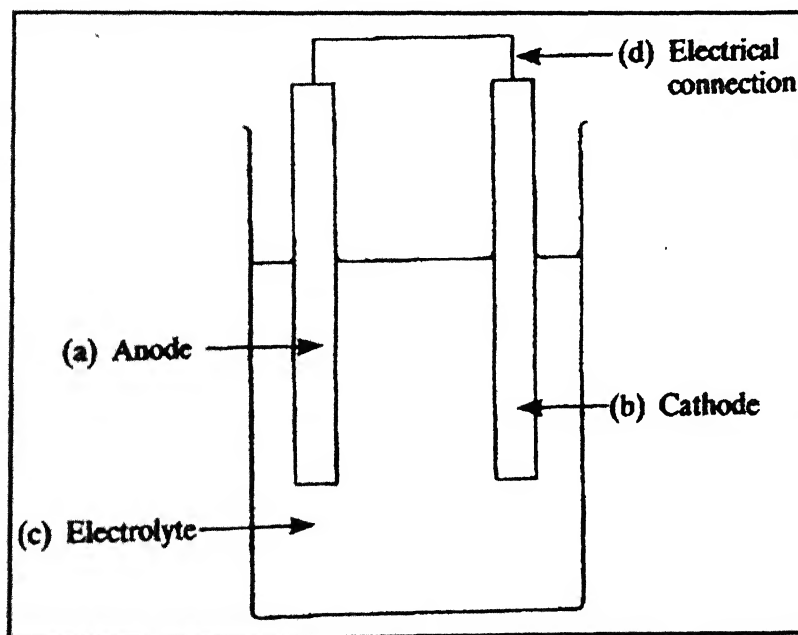
Figure 9 Basic wet corrosion cell [53].

Table 1: Standard reference electrode potentials [54].

Electrode	Electrolyte	Potential (V)
Calomel (SCE)	Saturated KCl	+0.2420
Calomel (NCE)	1.0 M KCl	+0.2810
Calomel	0.1M KCl	+0.3335
Silver/solver Chloride (SSC)	1.0 M KCl	+0.2224
SSC	Sea water	+0.25 (approx)
Copper/Copper sulphate (CSE)	Sea water	+0.30 (approx)
Zinc	Sea water	-0.79

2.5.1. Polarization

When a metal is not in equilibrium with the solution of ions, the electrode potential differs from the free corrosion potential by an amount known as the polarization [53]. It can also be said as overpotential or over voltage. Polarization is a very important corrosion parameter as it is useful in calculating the rates of the corrosion process. The deviation of the equilibrium potential is a combination of an anodic polarization of metal and a cathodic polarization of the environment. If the electrons are made available as in equation 5, the potentials at the surface become more negative, suggesting that excess electrons with their negative charges accumulate at the metal/solution interface waiting for the reaction. This negative potential charge is called as cathodic polarization. Similarly, there will be a deficiency of electrons on the metal surface interface by the reaction shown in equation 4, which produces a positive potential change called anodic polarization [54]. In an aqueous electrolyte solution the surface will reach a steady potential, E_{corr}, which depends on the ability and rate at which electrons can be exchanged by the anodic and cathodic reactions. When the surface potential increases above the E_{corr} value, to a value E, then the anodic polarization is given by the difference between E and E_{corr}. At equilibrium the forward anodic reaction, i_a is equal to the reverse cathodic reaction, i_c. Hence the rate of the reaction can be given by,

$$i_a = i_c = i_0 = A_o \exp[-\Delta G/RT] \tag{9}$$

There are two methods available for measurement of corrosion rate using polarization methods, namely Tafel extrapolation and polarization resistance. The polarization methods to measure corrosion rates have their inherent advantages. The main advantage of these methods is that the time taken for conducting experiments is relatively short, whereas the conventional weight loss methods require several days. The polarization methods are highly sensitive, and accelerating factors such as elevated temperature, to increase rates is generally not necessary. Moreover these methods are non destructive and several repetition experiments can be carried out using the same sample.

The mixed potential theory forms a basic for explaining the polarization techniques. The mixed potential theory consists of two simple hypothesis:

1. Any electrochemical reaction can be divided into two or more partial oxidation and reduction reactions.

2. There cannot be net accumulation of electrical charge during a chemical reaction i.e., corrosion reaction the sum of the anodic oxidation currents should be equal to the sum of the cathodic reduction currents. In other words the total rate of oxidation should be equal to total rate of reduction [55].

Consider the reactions for zinc getting corroded in an acid solution. Then the anodic and cathodic reactions are given by,

$$Zn \longrightarrow Zn^{2+} + 2e^- \quad \text{(Anodic reaction)} \qquad (10)$$

$$2H^+ + 2e^- \longrightarrow H_2 \quad \text{(Cathodic reaction)} \qquad (11)$$
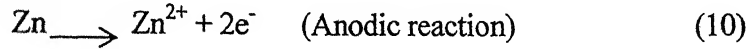
These reactions are called as the half-cell reactions and the potential corresponding to them are called cell potential. The potentials cannot coexist separately on an electrically conducting surface. The potentials will polarize to an intermediate value called as the corrosion potential or mixed potential (E_{corr}). When there is no external current flowing into the system, then the equilibrium potential attained is called open current potential (OCP) or free corrosion potential (E_{corr}). As the reactions polarize on the same surface the change in potentials is given by,

$$\eta_a = \beta_a \log (i_a/i_o) \qquad (12)$$

$$\eta_c = \beta_c \log (i_c/i_o) \qquad (13)$$

where η_a and η_c are anodic and cathodic polarization, β_a and β_c are the Tafel constants, i_a and i_c are the anodic and cathodic currents respectively. At E_{corr} the rate of anodic and cathodic reactions are equal and is equal to the current density, i_{corr}. The half-cell reactions for dissolution of Zn in acid are shown in the Figure 10 [53]. This figure is called as Evans diagram and represents an active material.

The various polarization techniques that are commonly used are linear polarization, Tafel extrapolation, potentiostatic polarization and cyclic polarization. These four polarization techniques are summarized in the Figure 11[56].

2.5.2. Potentiodynamic polarization

The potentiodynamic polarization is carried out in a wider range of potential spectrum and gives much more details about the samples response to the environment. The potentiodynamic polarization provides data about the metal behavior i.e., whether the metal

33

is active or passive or active passive in the given environment. The plot elucidates the properties of the passive film and the effect of inhibitors on the corrosion behavior of the metal. Depending upon the nature of potentiodynamic polarization curve, alloys can be divided into active alloys and active-passive alloys. For an active metal the corrosion rate increases linearly with increase in the anodic polarization potential. This is due to the non-protective oxide layer, which forms on the metal surface. For an active passive metal the corrosion rate increases with polarization potential upto a critical current density, (i_{crit}) after which it falls down rapidly due to the formation of a protective passive film.

A typical potentiodynamic polarization plot is shown in Figure 12 for an active passive metal [57]. The figure shows the various regions of a potentiodynamic plot for an active-passive metal. The first two regions are the normal cathodic and anodic polarization regions that were discussed for the Tafel plot. The anodic region is widened to show the passive film formation. The anodic region can be subdivided into three main regions namely, the active region, the passive region and the transpassive region. The active region and the cathodic curve can be extrapolated to extract the values of E_{corr} and i_{corr}. The active region ends at the primary passivation potential (E_{pp}) at which the passive film becomes stable and the corrosion rate falls rapidly. The current corresponding to this value is called as critical current density (i_{crit}). As the potential is increased beyond this value, the current density decreases until it reaches a steady current called as the passive current density (i_{pass}). The range over which the steady current is maintained is known as the passive range and it relates to the stability of the passive film. As the potential is increased further the passive layer breaks down and the anodic rate increases in the transpassive region. This breakdown in passivity can be attributed to the oxygen evolution or due to localized mechanisms such as pitting. In certain kind of alloys like stainless steel, there will be an additional region showing secondary passivity. This results due to the formation of some secondary oxide layer, which ultimately breaks leading to increase in the corrosion rate. The potential at which the passive film breaks is known as pitting potential (E_{pitt}) and the potential at which the oxide film completely breaks apart and is called the breakdown potential (E_{break}).

The schematic diagram in Figure 13 shows the type of alloy that can be used depending upon the nature of the environment. The figure shows four types of alloys and
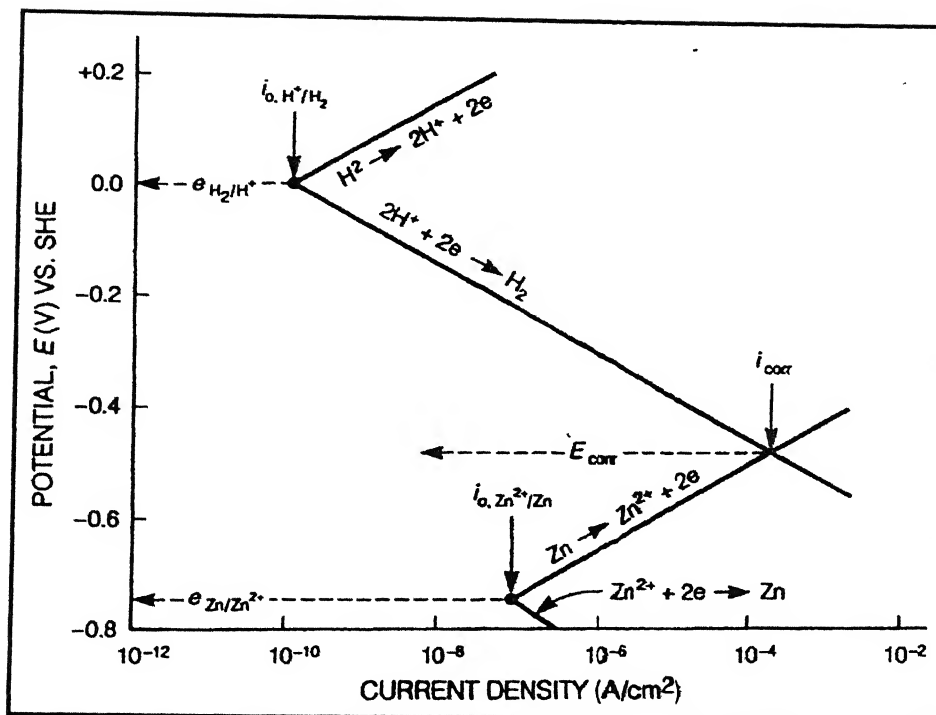
34

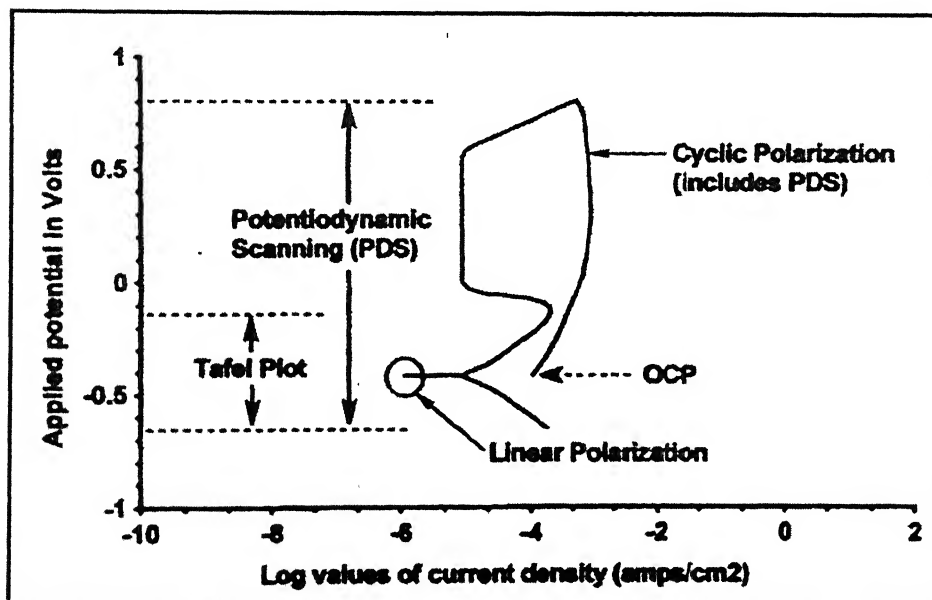Figure 10 Evans diagram for an active metal [53]

Figure 11 Various types of polarization methods [56].

three environments that are commonly used. For a reducing atmosphere, as in 1, either the non-passivating alloy A or the partially passivating alloy B is superior because they have better corrosion resistance in the active conditions. The alloys C and D produces strong passivity and hence alloying elements like chromium should be added. This makes the alloys more expensive and thus unjustifiable for the service condition [54]. For a moderately oxidizing atmosphere, number 2, the alloy C would be recommended because the reduction curve exceeds the critical current density and it is the only alloy showing stable passivity. In alloy B, the reduction curve exceeds critical current density, but the passive region is not broad enough to ensure good passive resistance. Alloy D is in a state of borderline passivity, with both active and passive states possible. For strong oxidizing condition in 3, alloy D is recommended as the reduction curve exceeds critical current density and the corrosion rate is low. In alloy C, the passivity breaks in this condition and it is in the transpassive region. Alloys A and B are not resistant to high oxidizing conditions. The main limitation of potentiodynamic polarization that the sample surface gets disturbed after the experiment is completed. Hence the test can be conducted only once at a time. Moreover the exact corrosion rate cannot be predicted accurately by this method.

2.5.3. Corrosion behavior of Metal Matrix Composites.

Though lot of research is done on the fabrication and mechanical testing of metal matrix composites (MMC), more emphasis is now given on the measurement and evolution of their corrosion behavior.

The corrosion rate of a metal system consisting of two dissimilar phases could reasonably be expected to be different from that of either phase alone. Local inhomogeneities in composition, structure, and stress could result in increased environmental attack of either phase and bring about the deterioration of the composite bond. In addition, when the reinforcement phase is a conducting material, galvanic coupling with the matrix would result in a greater dissolution rate of the more active phase. Since galvanic corrosion is generally observed at metal-metal contact points [58] this phenomenon would also affect the composite bond. Naturally, these problems would produce a serious degradation of the desired mechanical properties.
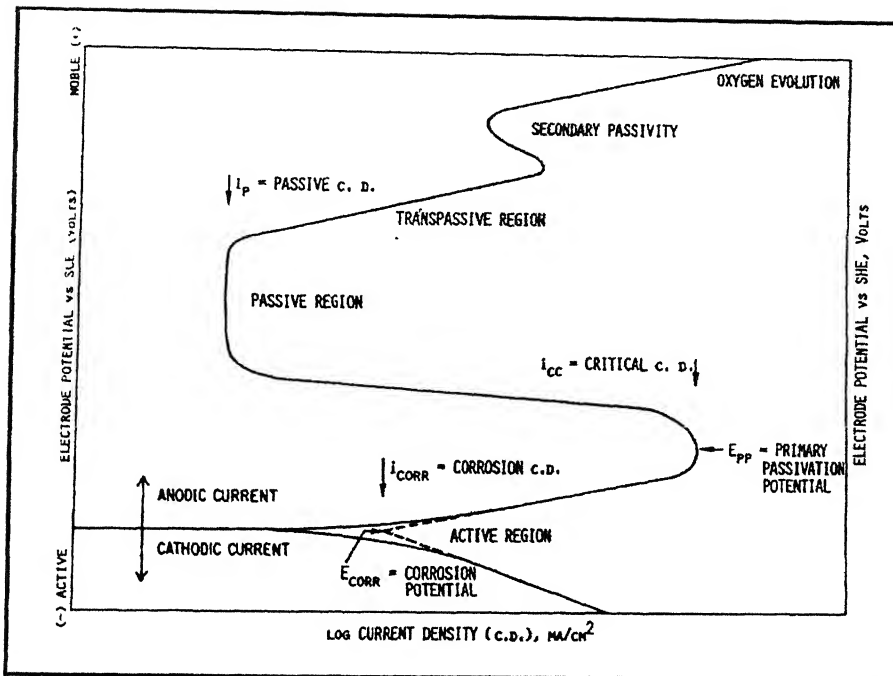
Figure 12 Schematic diagram show the potentiodynamic polarization for an active-passive metal [57].
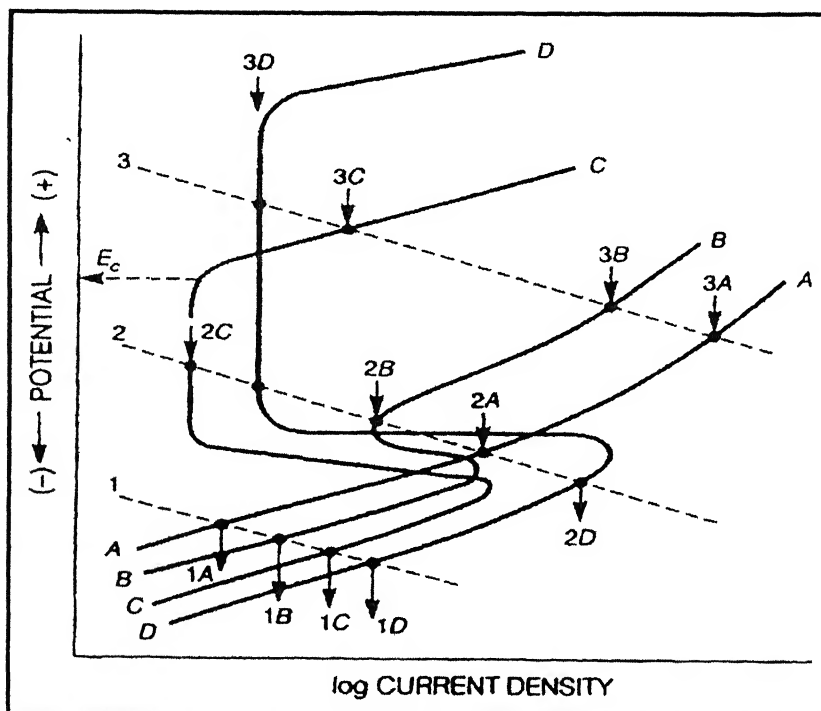

Figure 13 Anodic polarization curves for hypothetical alloy A, B, C, D in 1) reducing 2) moderately oxidizing 3) highly oxidizing environments[54].

Most of the research is being done on the aluminum matrix composite. As per author's concern, there is no literature available on the corrosion behaviour of Ni matrix composites. Evans and Braddick [59] studied the corrosion behavior of fiber-reinforced Al composites and compared with that of the Pure Al and an Al alloy. Although similar corrosion rates were found on the alloy and composite in their study, the modes of attack were different. Denise and Patrick [60] studied pitting behaviour of the Al-SiC composite and observed that the pitting was concentrated predominantly at the Al- SiC interfaces, with the pits being greater in number, smaller in size, and more shallow in penetrating depth relative to the non reinforced 6061Al alloys. Saxena *et al.* [61] reported higher corrosion rate of the composite than the base alloy in marine and acidic environments due to galvanic attack caused by these environments at the graphite-Al interface and the wicking effect of the electrolyte by the dispersed phase.

2.6. Tribology Fundamentals

Tribology is referred to as the science and technology of friction, wear and lubrication. Friction and wear are consequent events and lubrication can be considered as a tool to control these two. Friction and wear are two side of the same coin. Both are the result of one solid rubbing against another.

Friction leads to undesirable energy dissipation in machines of all sorts. The friction in an automobile engine for example leads to a loss in fuel efficiency and poorer miles per gallon. At the same time, frictional energy dissipation leads to local heating. The resulting local temperature rise can cause bearings to "burn out", plain carbon steel drills to become "over-tempered" and racing tires on Indy cars to fail. Nevertheless we rely on friction for the success of many applications. Without high friction materials we could not have brakes with stopping power, clutches would slip, tires would skid and shoe soles would fail to give us traction.

There are three fundamental friction laws, which are described as follows [62]:

1. $F_s = \mu P$ where F_s is the frictional force on the material in a direction parallel to the interface on which sliding has occurred or will occur and μ is a coefficient of friction. The friction can either be static (where F_s is the maximum force before the block starts to slip) - static friction coefficient = μ_s - or kinetic (where F_s is the force needed to continue the

sliding at a constant velocity) - kinetic friction coefficient = μk. The kinetic friction coefficient is always less than the static friction coefficient, i.e., $\mu k < \mu s$.

2. The second law states that the friction force (or coefficient of friction) is independent of apparent area of contact between the contacting bodies. Thus two bodies, regardless of their physical size, have the same coefficient of friction.

3. A third law of Coloumb's states that the kinetic friction force (or coefficient of friction) is independent of sliding velocity once motion starts.

In general, the surfaces of contacting bodies have microscopic bumps or asperities. These asperities arise from whatever was last done to the surfaces; processes such as machining, rolling, forging, grinding and polishing all leave asperities. Those left by polishing have smaller amplitude than those left by machining, for example, but such asperities are still present.

Wear is the effect of friction on material surfaces that rub together. Wear leads to loss of tolerances between mating parts and ultimately leads to failure of the system that depends of proper operation of these parts. However we rely on wear processes to grind and finish parts to their final shape. Every time we write with chalk on a blackboard or with a pencil on paper, we depend on wear processes to make our mark.

Wear occurs by mechanical and/or chemical means and is generally accelerated by frictional heating. Principal wear mechanisms involved include adhesive, abrasive, fatigue, erosion, chemical and fretting and combinations of all or any of these. In many cases, wear is initiated by one mechanism and it may proceed by other wear mechanisms, thereby complicating failure analysis [63].

Fretting occurs where low-amplitude oscillatory motion (a few tens of nano-meters to a few of tens of micrometers) takes place between contacting surfaces, which are nominally at test. A rapid increase in wear rate occurs with slip amplitude over an amplitude range [63]. Basically, fretting is form of adhesive or abrasive wear, where the normal load causes adhesion between asperities and oscillatory movement causes ruptures, resulting in wear debris. Most commonly, fretting is combined with corrosion; in which case the wear mode is know as fretting corrosion. Fretting occurs between prosthetic hip joints and bone, gear and shafts, transformer cores and in many other places. It loosens some joints, seizes up others and may provide a site for crack initiation.

To reduce friction, we introduce a material between asperities that slides over it self easily. This material has to also withstand high pressure between asperities and adhere to the sliding surface otherwise it will be squeezed out or rubbed off and we will be back to the same problem. Modern lubricants are oils, greases and fatty acids - short chain polymers ("oligomers") that "contaminate" surfaces and slide easily over each other. They also contain additives that attach to metal or ceramic surfaces. Such molecules have polar heads and hydrocarbon tails - the head "grabs" the surface and the tail bonds only weakly, by vanderWaals bonds, to the surrounding lubricant. The additive-coated surface slides easily past the lubricant molecules.

Successful electrodeposition of graphite-brass composite coatings and subsequent characterization of tribological properties were done by Ghorbani *et al.* [64]. Composite coating was observed to be having mono phase matrix (α-brass) and graphite particles. The graphite content in composite influences the weight loss in the wear test and coefficient of friction of composite coating depends on graphite content, load, distance and speed in the wear test. The graphite containing approximately 3.7 vol. % graphite was found to be having the best tribological properties.

Garcai [65] *et al.* studied the friction and wear behaviour of electro-codeposited SiC particles of 5, 0.7 and 0.3μm sizes from Watt's solution with uni and bi-directional sliding against corundum balls. And they obtained best sliding resistance with Ni-SiC composite coatings containing 4-5 vol. % submicron SiC particles.

In the study of K.H. Hou [6] *et al.*, an attempt has been made to investigate the wear resistance of Ni-SiC composites manufactured by electro-codeposition process, which is significantly correlated to the vol. % SiC in the matrix. In addition, the contents of submicron-size SiC particles in the deposition layer increased with the increasing concentration of both the SiC and the surfactant CTAB in the electrolyte. It was found in their investigation that the surfactant CTAB can not only disperse the SiC particles well in the electrolyte therefore leading to better homogeneously distributed SiC particles in the matrix but also enhances the SiC vol.% embedded in codeposition layer. It was confirmed that the wear resistance of codeposited layer increase with increasing submicron-size vol. % SiC.

Chapter 3

Experimental Procedure

3.1. Materials

The plating solution used was a standard nickel Watts' solution of pH 4.0. The composition of the plating solution and the plating parameters are given in Table 2. Tungsten Carbide (WC) particle with average size of 5 μm was used. "Fritsch particle sizer analysette 22" was used for analyzing WC particle size (Figure 14). The particle concentration in the plating solution was 2 g/l. 1.5 X 1.5 cm^2 out of 2 ×1.5 cm^2 Mild steel plate was immersed in the electrolyte to obtain the deposit. Pure Ni was used as anode.

3.2. Equipment

A Julabo F-32 temperature controller was used to control the temperature during experiment, which has an accuracy of ±0.2^{0}C. A Magnetic stirrer (Remi 2 LH type) was used to homogenize the bath. The cell (a beaker of 250 ml capacity) had inlet and outlet connections to maintain the bath temperature. A Teflon-coated stirring rod (8 mm dia, 30 mm length) was placed inside the bath, which rested on the platform of a magnetic stirrer. The top of the cell was covered with the lid containing provisions for the introduction of the electrodes into the bath having electroplating solution and suspended WC powders. A constant DC regulatory power supply (model: SVP 100010) was used for passing the current.

3.3. Specimen Preparation

Mild steel flats of 2.5 X 1.5 cm^2 were polished on an emery belt. Water was used as the lubricant during polishing to decrease the heating of the specimens during polishing. After emery belt polishing, the specimens were polished on emery papers up to 4/0 finish on both sides. All the sharp corners and edges of the specimens were rounded off to avoid dendritic deposition at the corner place. The specimens were finally ultrasonically cleaned with acetone to remove any grease on the surface.

Table 2. Plating parameters and Composition of the plating solution.

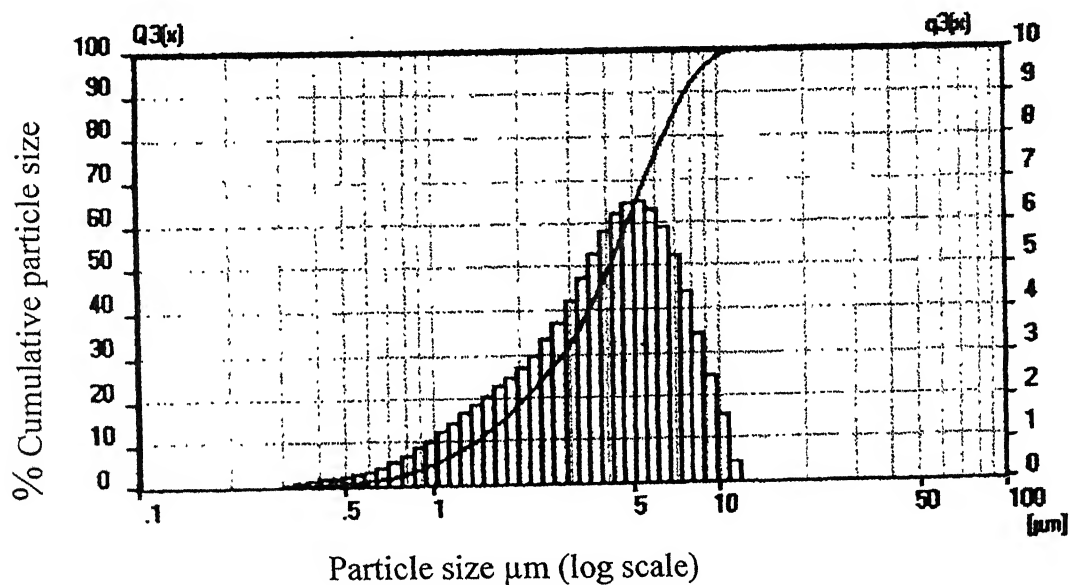| Component	Bath composition	Parameters	Condition
		Temperature	50^0 C
NiSO$_4$ 6H$_2$O	250 g/l	pH	4.2
NiCl$_2$ 6H$_2$O	35 g/l	Current Density	0.1, 0.2, 0.3,
H$_3$BO$_3$	40 g/l	Stirring rate	300 rpm
WC particle (10μm)	2 g/l	Stabilisation time	2 hr
		Cathode:	Mild steel
		Anode:	Pure Nickel

Figure 14 Shows the WC particle size analysis.

3.4. Procedure

A schematic diagram of the setup used in the present study is shown in Figure 15. All experiments were carried out with 125 ml of the electrolyte. The temperature of the plating solution was slowly raised till it reached 50^0C, and then the measured quantity of WC powder particles was added to the plating bath. The bath was blended for one hour. Electrodeposition was carried out on vertical electrodes, and the plating solution was agitated during electrodeposition with a magnetic stirrer. This was done to ensure uniform suspension of particles in the bath. The stirring was maintained at the laminar flow conditions (350 rpm). Just after the blending period was over, the electrodes were introduced into the bath with the help of the specimen holders and the power supply was switched on allowing the required current to pass through the circuit. The plating time was 15 minutes in all the cases. Distilled water was added to makeup the evaporation loss, if any, during the course of the experiment.

At the end of the experiment, the cathode was taken out and washed with water. The specimen was dried and weighed in an analytical balance (Anamed, MX 7301A model). The weight percentage of co-deposited Ni and WC were found by weight analysis. The solution was filtered through a previously weighed G4 crucible. Electrolyte comes out through the filtrate and WC stays within the crucible. WC in the crucible was washed with water and then dried in an air oven kept at 100^0C for an hour. The crucible was partially allowed to cool in air and then cooled down to room temperature in a desiccator. The difference between the final and initial weight of the WC in the solution gave the weight of WC in the coating. The weight of the composite coating was determined from the weight gain of cathode. Knowing the weight of the WC deposited, the weight of Ni deposited was calculated. The subsequent weight percentages of Ni and WC were calculated from the obtained weights. The theoretical weight of deposited Ni was calculated by using Faraday's laws of electrolysis from the result of which, the cathode current efficiency was found.

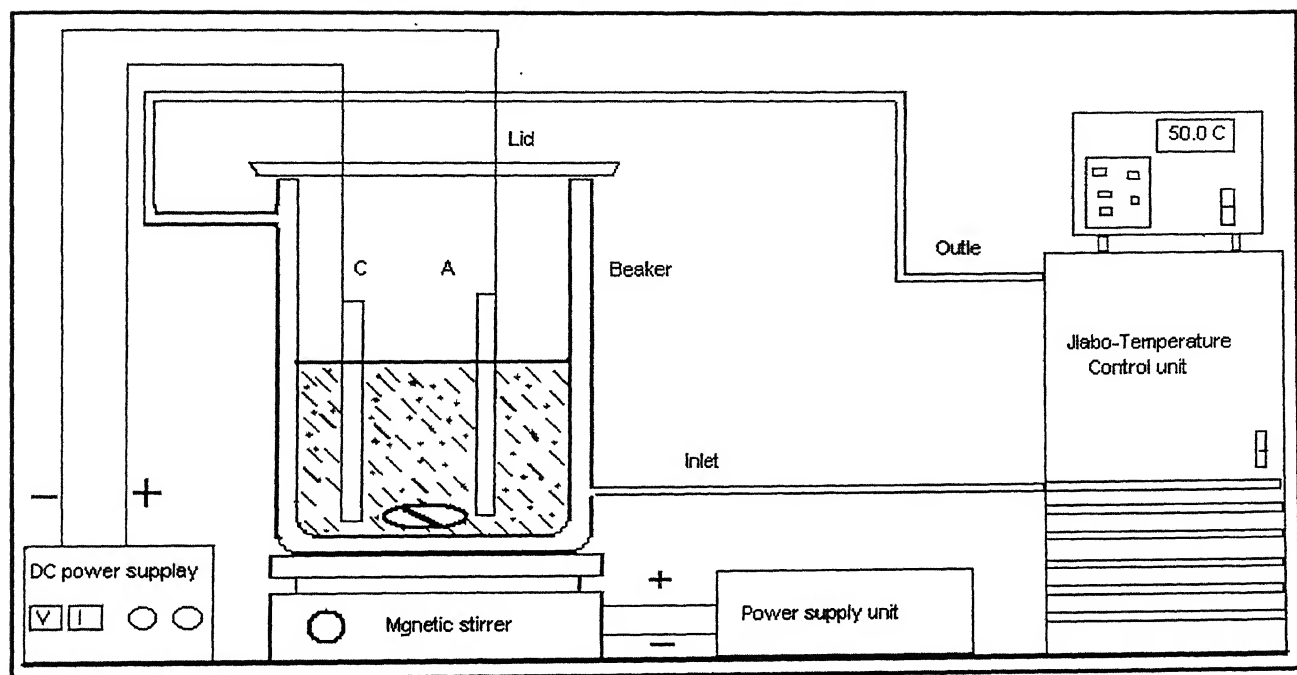$$W_{th} = \frac{E \times I \times t}{F} \qquad (14)$$

Figure 15 Schematic diagram showing the experimental arrangement for the electròdeposition study.

where W_{th} = Theoretical weight of deposited Ni in gm, I = Current passing through the cathode, in amps, t = Duration of plating in sec, F = Faraday's constant, E = Equivalent weight of Ni,

$$\text{Cathode current efficiency, } \eta = \frac{W_{actual}}{W_{th}} \times 100 \qquad (15)$$

were W_{actual} = Actual weight of deposited Ni in composite coating. "Rule of mixture" was used to calculate the density of the composite coating. After deposition, some of the samples were cut and mounted in epoxy resin. Metallographic cross-sections for optical and SEM observation were ground and polished by using SiC abrasive paper.

3.5. Microstructural Characterization

The microstructures of the as deposited cross-sectioned samples were studied by optical microscope (Axiolab A, Zeiss, Germany) and scanning electron microscope (SEM) (JEOL JSM 840A). Standard metallographic techniques used for preparation of the samples were mounting, grinding and polishing. A diamond wheel cutter (Buehler-ISOMET) was used for sectioning the specimens. The diamond wheel was operated at a relatively low speed in order to avoid any damage of the sample and the cutter. The specimens were hot mounted. Care was taken while mounting to maintain the flatness of the sample and mount. Grinding of the sample was performed in a series of emery papers starting from coarse grit to fine grit. The sample was ground carefully to avoid higher relief of the softer matrix than the hard carbides. Polishing was performed by using 0.5 μm alumina powder. For revealing the microstructure, Merica solution was used as etchant (50/50 nitric and acetic acids) [66].

3.6 Microhardness Measurements

Microhardness measurement of the both the composite coated layer of all the sample were performed using a microhardness tester (Carl Zeiss, Jena, Jenavert, German) attached with an optical microscope. A diamond pyramid indenter with a 20 g load was

employed and observations were made at magnification of 200X. All the values were noted as Vickers hardness number (VHN) which was obtained from the formula written below:

$$VHN = \frac{1854.4 \times P}{d^2} kg/mm^2 \qquad (6)$$

where P is the load in grams and d is the average of two diagonal of indentions mark in micro-meter.

3.7. Electrochemical Characterization

3.7.1 Corrosion potential stabilization

Electrochemical polarization studies were conducted using a Perkin Elmer potentiostat (model 263A). Its ±20 V compliance and ±200 mA (±2 A with 94 Option) output capabilities allowed rapid and accurate potential or current control in the electrochemical cell. The schematic of a potentiostat connected with the polarization cell is shown in Figure 16. The potentiostat consist of ammeter, an electrometer and a power supply. Three probes from the potentiostat were connected to the working electrode, reference electrode and counter electrode. The fourth probe was ground. The polarization cell used for the polarization studies was the flat cell. The schematic representation of the cell is shown in Figure 17. The flat cell was used in the present study. An Ag/AgCl electrode in saturated KCl was used as the reference electrode and the counter electrode was a platinum grid. The potential of the reference electrode was +222 mV with respect to standard hydrogen electrode (SHE). The working electrode was placed in the flange and tightened so as to expose only 1 cm^2 of the sample area to the electrolyte. The sample did not require any type of polymer mounting for this type of cell, as there was provision for attaching the sample without mounting. However, both the surfaces of the sample should be flat in order to prevent leakage of electrolyte.

The test was conducted in 0.1 mol/liter. H_2SO_4 solution. The solution was prepared using distilled water and laboratory grade chemicals. The surface of all the samples that were exposed in electrolyte were polished up to 4/0 emery paper and the sample were tested in the flat cell.
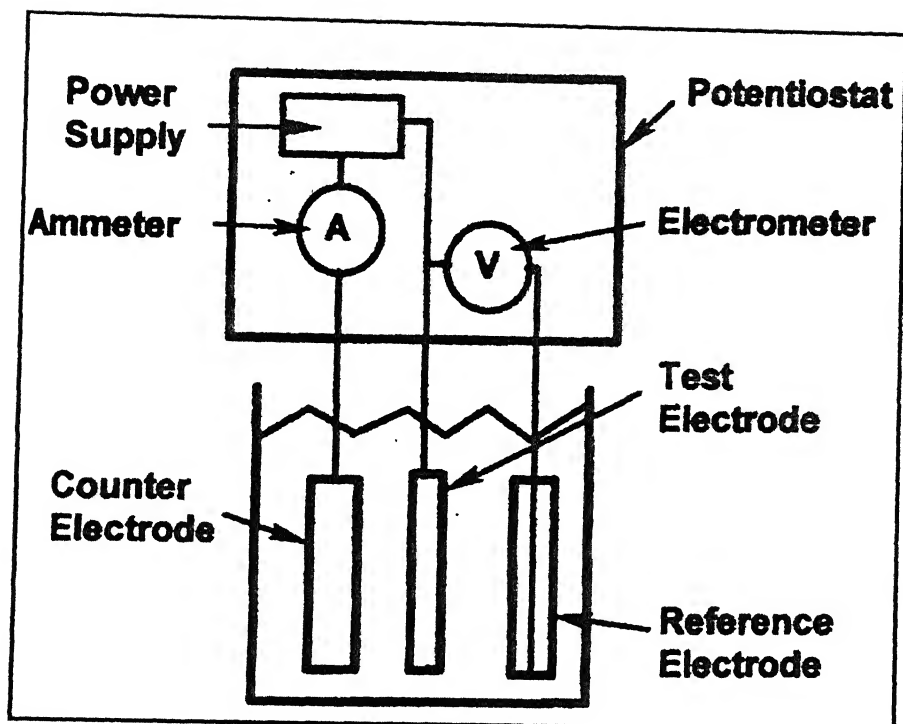
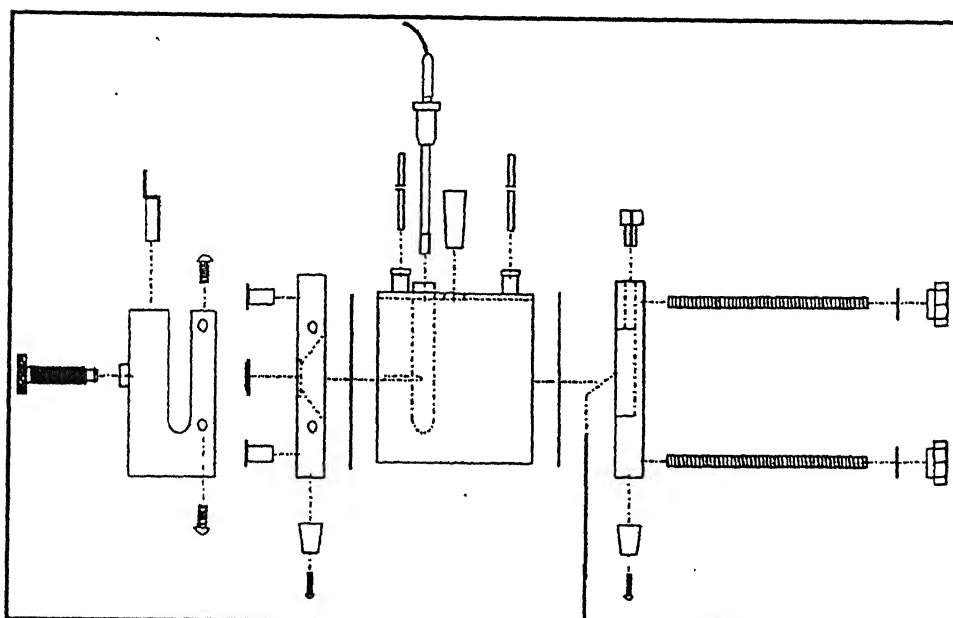Figure16 Schematic diagram shows the connection in the potentiostat.

Figure 17 Schematic representation of flat cell.

3.7.2 Potentiodynamic polarization

The potentiodynamic polarization experiment was carried out in the range of -500 mV to +1600 mV for all samples. The experiments were started immediately after fixing the specimens in flat cell. This prevents the formation of the surface film before experiment was started. This also allowed comparison of i_{crit}. All potentiodynamic experiments were carried out at scan rate of 1 mV/sec.

3.8. Wear Test

For the tribological testing of the investigated Ni-WC composite, a commercial ball- on- flat fretting wear (low amplitude reciprocatory tangential sliding) tester (Figure 18) is used in this research. An inductive displacement transducer monitors the displacement of the flat sample, and friction force is recorded with piezoelectric transducer attached to the holder that supports the counter body. The friction coefficient is obtained from the on-line measured tangential force.

The as-deposited and polished Ni-WC coated samples were used as flat (moving) materials. 6 mm diameter bearing grade (commercial SAE 52100 grade) steel ball was used as a counter body (stationary). Prior to the fretting tests both the flat and ball were ultrasonically cleaned in acetone. To investigate the coating performance over extended time duration, some tests were carried out with critical sliding conditions. Reciprocatory sliding ball-on-flat wear tests [67] were performed at a normal load of 1 N, an oscillation frequency of 8 Hz, and tangential displacement amplitude of 100 μm. The number of fretting cycles was 10,000. All wear tests were performed without lubrication, at room temperature and in ambient air of 40% relative humidity. The coefficient of friction was recorded continuously during the wear tests. After completion of the wear tests, all samples were cleaned in ethanol using ultrasonic agitation for 5 min and optical microscope analysis was done on the scars. This combination of fretting parameters results in the linear sliding speed of 0.0016 m/s. All the wear tests were done at room temperature. The test parameters are summarized in Table 3.
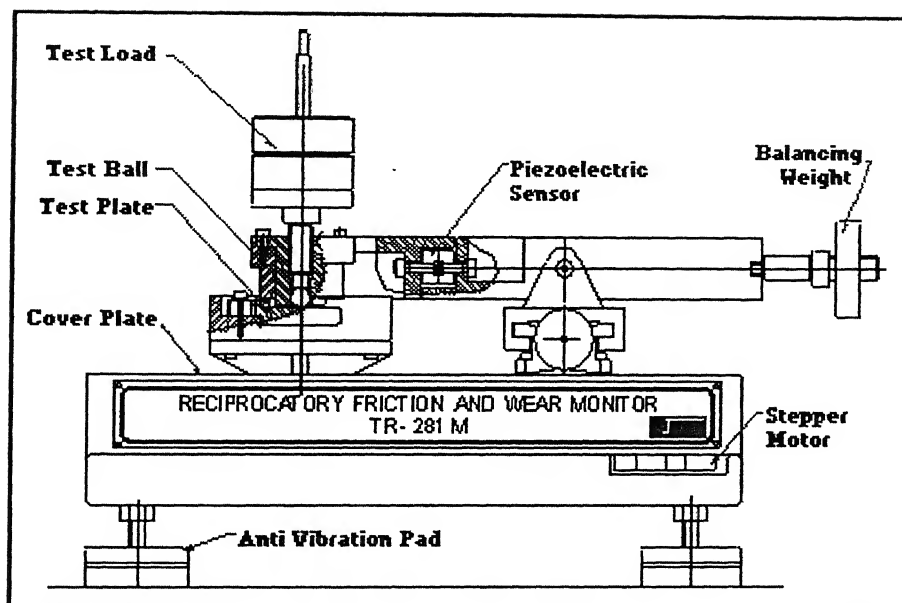
Figure 18 Schematic of the fretting wear tester, manufactured by DUCOM, India.

Table 3: Various fretting test parameters.

Parameter/variable	Value
Temperature	Room Temperature
Load	100 g
Cycles	10,000
Stroke Length	100 μm
Frequency	8 Hz
%R.H	40

3.8.1. Characterization of worn surfaces

Detailed microstructural characterization of the as-worn and ultrasonically cleaned (after wear tests) surfaces both on flat and ball was performed with a Leitz optical microscope. The wear behaviour of the composite coating under fixed fretting conditions was estimated by reporting COF.

Chapter 4

Results and discussion

4.1. Electrodeposition Characterization

The effects of the following variables were studied on the deposition of Ni-WC from Watts' bath. The plating period for all experiments was 1.15 hr and the specimen was of 1.5 x 1.5 cm^2 dimensions.

4.1.1. Effect of blending time

The blending time varied from 1 to 3 hr, and its effect on weight percentage of WC in coating was determined at constant current density, temperature, and deposition time. The distribution of WC in the composite layer and the nature of the as-deposited surface morphology were studied with optical microscope. It was observed that increase in the blending time had no effect on the distribution and surface morphology of composite coating. There was no effect of blending time on weight of deposition. The blending time was fixed for one hour. All further experiments were carried out by blending the WC in the bath for one hour with constant stirring such that all the WC particles were wetted and remained suspended uniformly in the electrolyte.

4.1.2. Effect of Temperature

Variation in the bath temperature at 0.2 A/cm^2 current density and constant bath load showed mixed trends with regards to the weight of WC in the deposit. Increase in weight of deposited WC was increased with temperature up to 50°C, while the amount of WC decreased with temperature above 50°C. Metallographic observations revealed that a uniform distribution of WC in the composite was obtained for deposition conducted at 50°C (Figure 19a-19c).
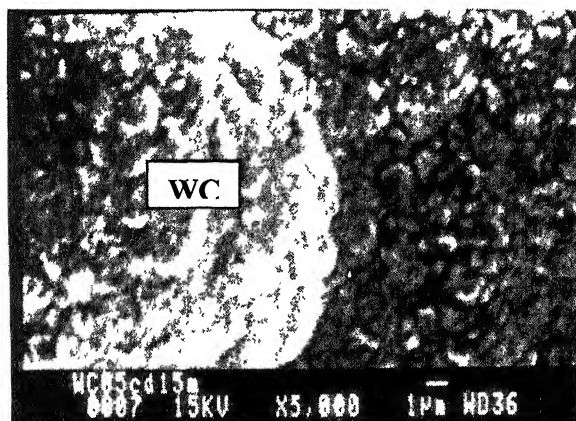
Figure 20 shows as-coated composite surface morphology at 0.2 A/cm^2 current density and 60°C temperature. The agglomeration of the particles due to the effect of high temperature can be clearly seen in these figures. At higher temperature the amount of WC
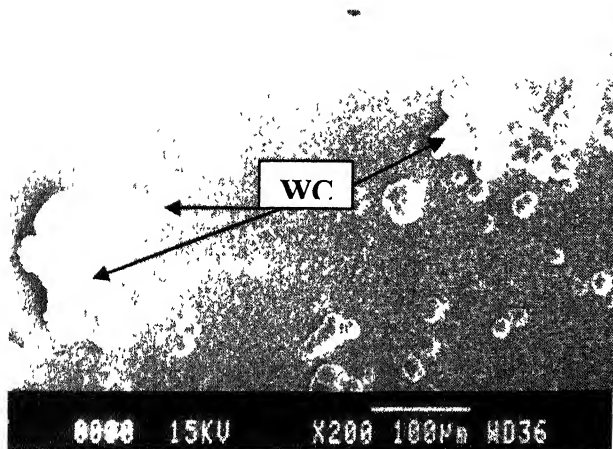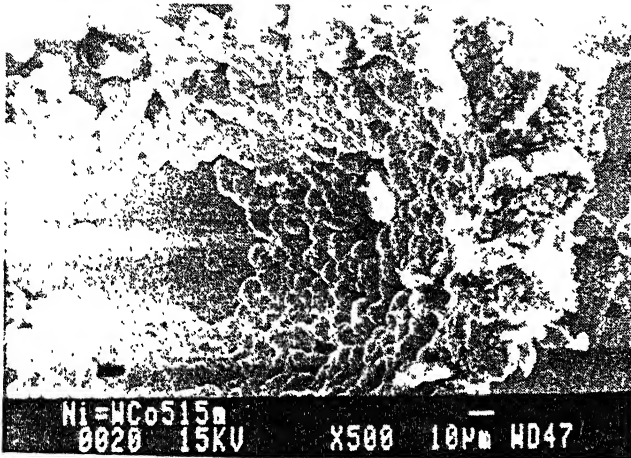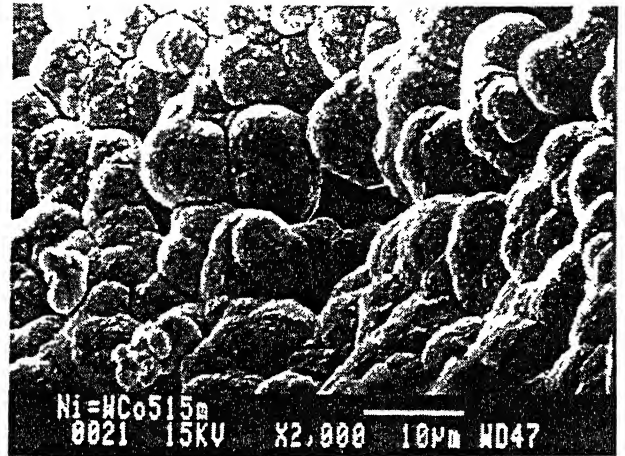
(a)
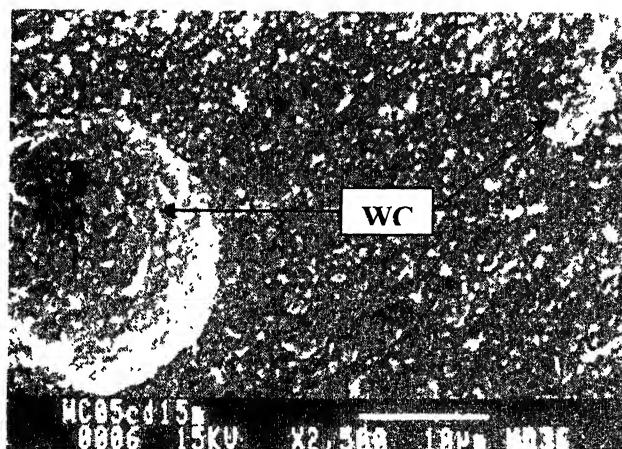
(b)

(c)

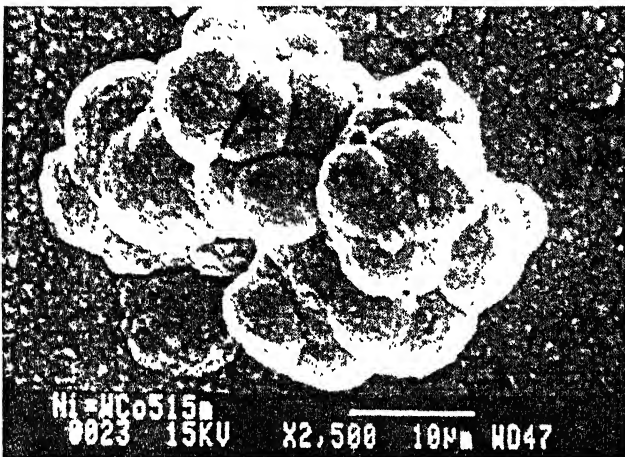Figure19 SEM micrographs showing as-coated composite surface morphology at 0.2 A/cm^2 current density, 50°C temperature and at constant stirring.
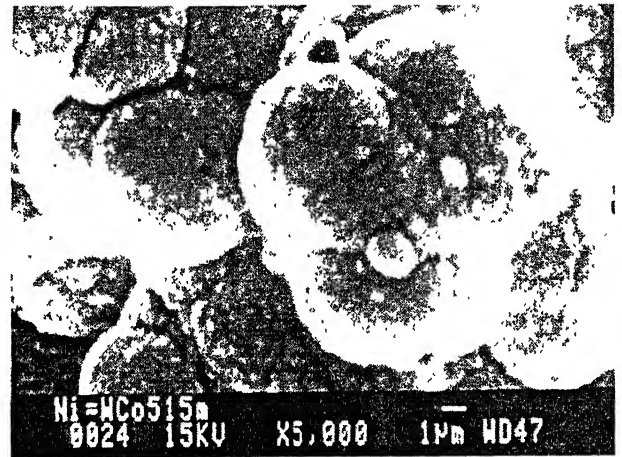
(a)

(b)

(c)

(d)

Figure 20 SEM micrographs showing agglomerated WC particles a) cluster of particles b) higher magnification c) agglomerated one on top of another d) same at higher magnification of c, (60^0C and 0.2 A/cm^2 in as-coated Ni-WC composite).

particles in the deposited layer decreases and the same was observed by Rajnarayan [52] and Chatopadyay in the Cr-Al$_2$O$_3$ composite coatings.

4.1.3. Effect of Current Density

As the current density was increased at a constant bath load of 2 g/l and temperature of 50^{0}C, the weight of WC in the composite coating decreased. These results are tabulated in Table 4. The deposit was adherent and continuous. The deposit was thicker at the center of the plate than at the corners for all current densities (Figure 21). The variation in thickens between the center and corner was observed to be higher at 0.1 and 0.3 A/cm^2 current densities. An almost uniform deposit thickness was obtained for deposition with 0.2 A/cm^2 current density. The adherent layer was quite non-uniform for deposits produced with highest current density, with higher amounts of protrusions being observed at corners as shown in Figure 22.

The cathode current efficiency increased with increasing current density. This must be related to increasing the amount of nickel in the composite coating with increasing current density (Table 4).

The distribution of WC particles in the composite coated layer with varying current densities is shown in Figure 23. These SEM micrographs reveal a more uniform distribution of WC particles at 0.2 A/cm^2 current density than at the other two current densities. Based on the above observation 0.2 A/cm^2 was taken as a current density to study the deposition at different bath loads. It is clear from these photographs that an increase in the current density decreases the amount of WC particles in the deposited layer. Figure 24 illustrates some cross-sections of the Ni-WC composite deposit indicating a smooth deposit and free of defects.

4.1.4. Effect of bath load

The effect of bath loads (2, 5, 8, and 10 g/l) was studied keeping all other deposition parameters constant with current density 0.2 A/cm^{2}and temperature 50^{0}C. The results of the study are presented in the Table 5. The wt% of WC in the composite was found to be 18.7 at lowest bath load of 2 g/l. and this increased with increase in bath loads reaching a maximum of 38.41 for the bath load at 8 g/l. The highest bath load of 10 g/l,

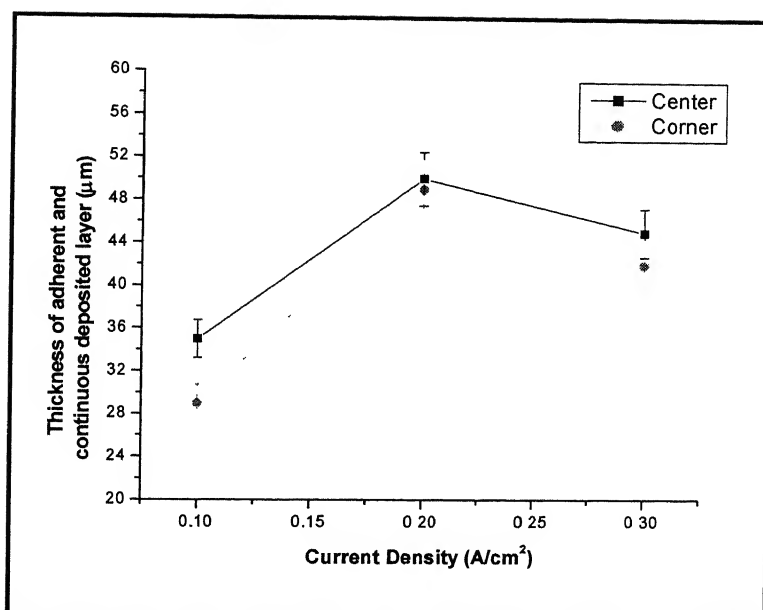Figure 21 Variation in thickness of Ni-WC composite coatings deposited at different current densities.
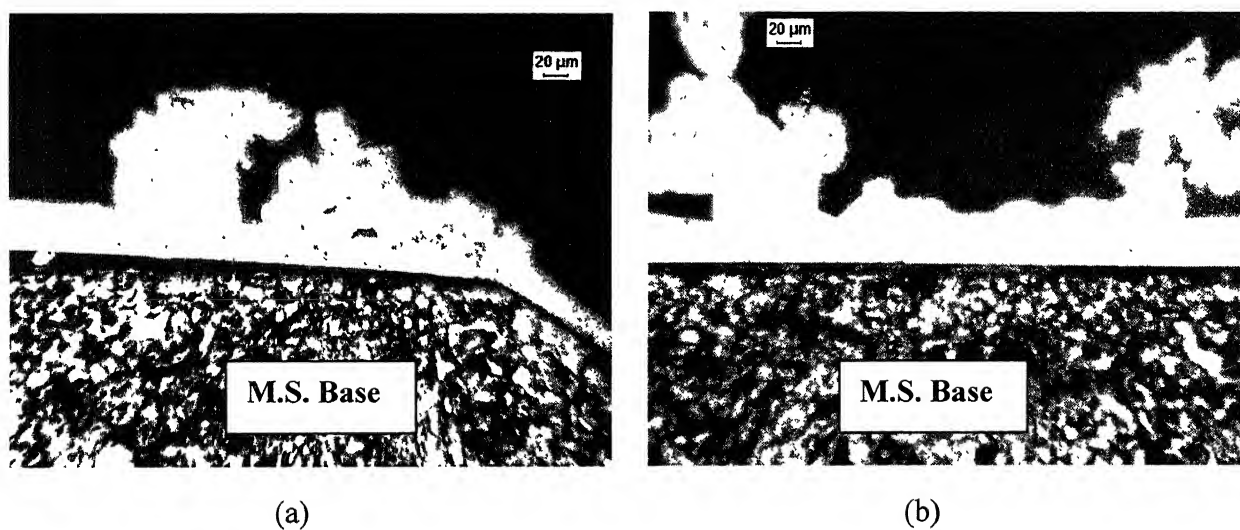

(a)   (b)

Figure 22 Optical micrograph shows the protrusions at 0.3 A/cm^2 current density a) corner and b) center.

Table 4: Effect of current density on deposition parameters, constant bath load 2 g/l and temperature 50^0C.

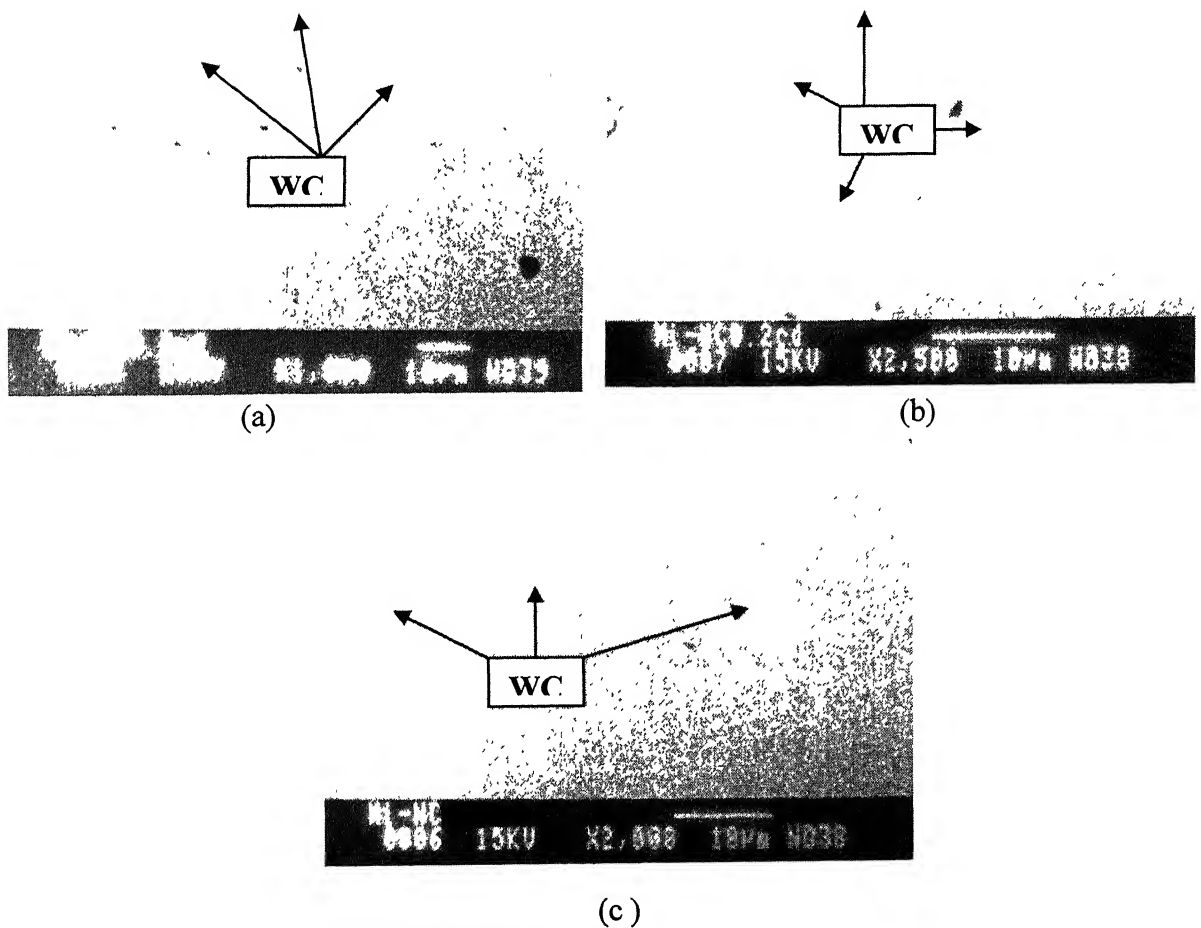| Current density (A/cm^2)	Wt % of Nickel	Wt % of WC	Thickness of the layer (μm)		Cathode Current Efficiency %
			Center	Corner	
0.1	63	36.99	35 ± 5	29 ± 4	66.35
0.2	81.29	18.70	50 ± 6	49± 4	74.87
0.3	90.15	9.85	45 ± 5	42 ± 6	99.43

(a)

(b)

(c)

Figure 23 Cross-section views of SEM micrographs showing the distribution of WC particle in Ni-WC composite coated layer at a) 0.1 A/cm^2 b) 0.2 A/cm^2 and c) 0.3 A/cm^2
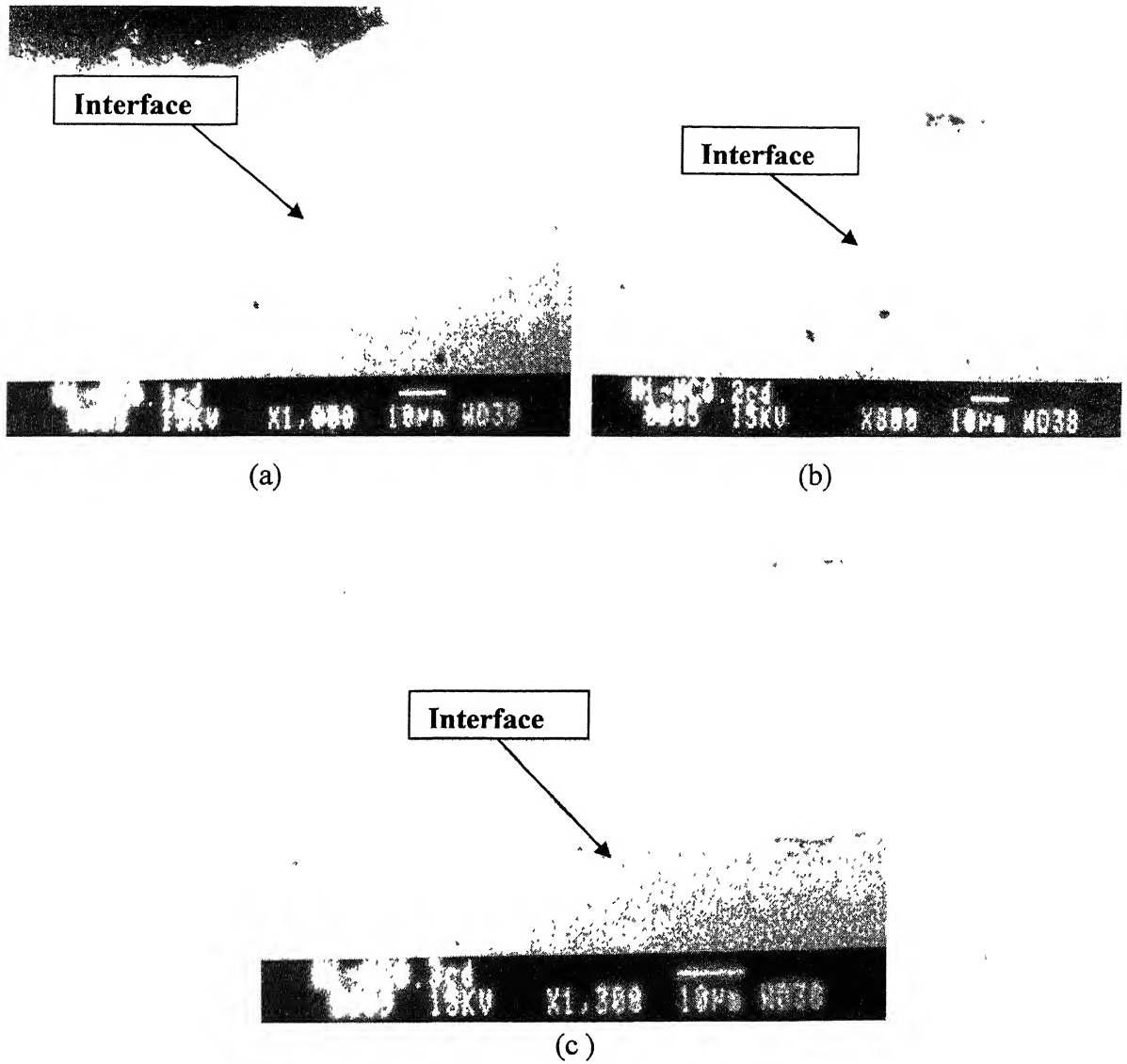
Figure 24 SEM micrographs showing the interface between base and coated layer of Ni-
WC composite at different current densities a) 0.1 A/cm^2, b) 0.2 A/cm^2, and c)
0.3 A/cm^2.

however, resulted in a decrease Wt% Ni (35.59). The bath load also affected the cathode current efficiency. The cathode current efficiency decreased with increasing bath load.

4.2. Microhardness

In order to understand the mechanical effect of the WC in the composite coating, microhardness tests were performed on the cross-sectioned deposited layer. The results are tabulated in Table 6. The effect of current density on the microhardness of the composite layer is shown in Figure 25, while the variation in microhardness as a function of WC content in the composite coated layer is shown in Figure 26. The microhardness increased with increasing WC content in the composite coating. The hardness increase noted in these composite coating can thus be linked to a dispersion-strengthening effect [65]. This indicates the importance of achieving a dispersion of WC particles to obtain a dispersion strengthening effect.

4.3. Electrochemical Behavior

The electrochemical behaviour of the composite coatings was studied by polarization methods. Electrochemical tests were conducted using a flat cell containing platinum as the counter electrode and Ag/AgCl as the reference electrode, all the potentials mentioned further is with respect to silver/silver chloride (SSC) reference electrode. Potentiodynamic polarization tests were conducted at a scan rate of 1 mV/sec commencing at a cathodic pretreatment potential of about − 400 mV (vs SSC) and terminating after reaching trasnpassive region at a potential of about 1600 mV. All the tests were conducted using ultrasonically cleaned test specimens. The electrochemical behavior of the Ni-WC composite coating was studied using 0.1 mole/lit H_2SO_4 solution as the electrolyte.

Figure 27 shows potentiodynamic polarization curves for coated composites and pure nickel. The composites were obtained by coating at different current densities, all the Ni-WC composites exhibited active-passive behaviour, typically observed in pure nickel in the 0.1 moles/lit H_2SO_4 electrolyte. However, some notable differences in polarization behavior were evident between the composites and pure nickel. The passivation parameters determined from the potentiodynamic polarization curves are tabulated in Table 7. The β_a, β_c and i_{corr} parameters from the experimental plot are tabulated in the Table 8.

Table 5: Effect of the bath load on weight of the composite coating and efficiency.

Bath load (g/l)	Wt of composite deposited (g)	Wt deposited		Wt% deposited		Cathode current efficiency %
		Ni (g)	WC (g)	Ni (%)	WC (%)	
2	0.304	0.246	0.058	81	19	83
5	0.354	0.232	0.122	65	35	78
8	0.322	0.198	0.124	61	39	67
10	0.295	0.105	0.19	64	36	35

Table 6: Microhardness of Ni-WC coated composite.

System	C.D A/cm^2	Micro-hardness (Kg/cm^2) (at different locations)						Average
Mild steel	-	186	170	181	176	168	188	178
Pure Ni	-	243	254	251	220	279	250	249
Ni-WC	0.1cd	270	357	317	333	333	322	322
Ni-WC	0.2cd	247	292	302	297	306	287	288
Ni-WC	0.3cd	230	297	240	283	292	230	262

There is difference in the apparent corrosion potential (E_{ZCP}) of these materials, with the Ni-WC composite coated system showing no specific trend in E_{ZCP} values. The free corrosion potential of Ni in acid media is largely governed by the characteristic of hydrogen evolution. Decreasing proton activity in solution or at the electrode surface, and hydrogen evolution kinetic, typically results in active (negative) shifts in E_{corr} [68]. The E_{corr} shifts depend upon the WC in the coating noted in this study and also may be due to catalysis of hydrogen reduction process by substantial quantity of crystalline defect (at grain boundaries) at the Ni-WC coated surface [68]. The exchange current density for the reduction reaction, assuming hydrogen reduction reaction, was determined from the polarization diagram and tabulated in Table 7. It is interesting to note a direct co-relation between the E_{ZCP} and exchange current density with increasing proton activity (i.e. increased i_0) the E_{corr} shift in the positive direction region, therefore this aspect needs to be investigate further. As a consequence, the Ni-WC deposit at 0.2 A/cm^2 current density would appear to be the least defective based on its low i_0 and also more negative E_{ZCP}. Based on the potentiodynamic polarization behaviour, it is evident that the principle influence of the WC in the Ni coatings on the electrochemical behavior of pure nickel is with regards to passivity. The Ni-WC composite structure apparently decreases the stability of the passive film which is evidenced by a positive shift in the passivation potential, reduction in the passive range, and substantially higher passive current densities.

4.4. Friction and wear behavior

In this chapter, the tribologial behavior of the Ni-WC composites, deposited at varying current densities is discussed. The friction and wear behaviour of the coated composites, fretting against bearing ball SAE52100 grade steel are shown in Figure 28.

In Figure 28, the coefficient of friction (COF) versus number of cycles is plotted for Ni-WC coated composites (0.1, 0.2, 0.3 A/cm^2 current densities), pure nickel and uncoated mild steel with constant testing parameters of 8 Hz frequency, 100 μm sliding distance, 1N load, and 10,000 cycles. The evolution of COF shows different behavior for both the coated and uncoated mild steel as well as for pure nickel. During the running-in-period of first 1000 cycles, COF increased from a low value to a very high value and

Table 7: Passivation and electrochemical parameters obtained from the potentiodynamic polarization curves of pure Ni and composite Ni-WC samples.

System	C.D. A/cm²	E_{ZCP} mV	E_{pp}	E_{cp}	E_b	E_b-E_{cp}	i_0 (H⁺/H₂) mA/cm²	i_{crit}	i_{pass}
Pure Ni	-	-128	12	360	1100	740	3.31×10^{-4}	2.75	0.03
Ni-WC	0.1	-68	270	347	724	377	4.36×10^{-3}	2.69	0.93
Ni-WC	0.2	-272	61	171	597	426	1.0×10^{-4}	1.81	1.25
Ni-WC	0.3	-138	388	475	996	521	2.13×10^{-3}	2.95	1.81

Table 8: Values of β_a, β_c and i_{corr} obtained from the potentiodynamic polarization curves of pure Ni and coated composites.

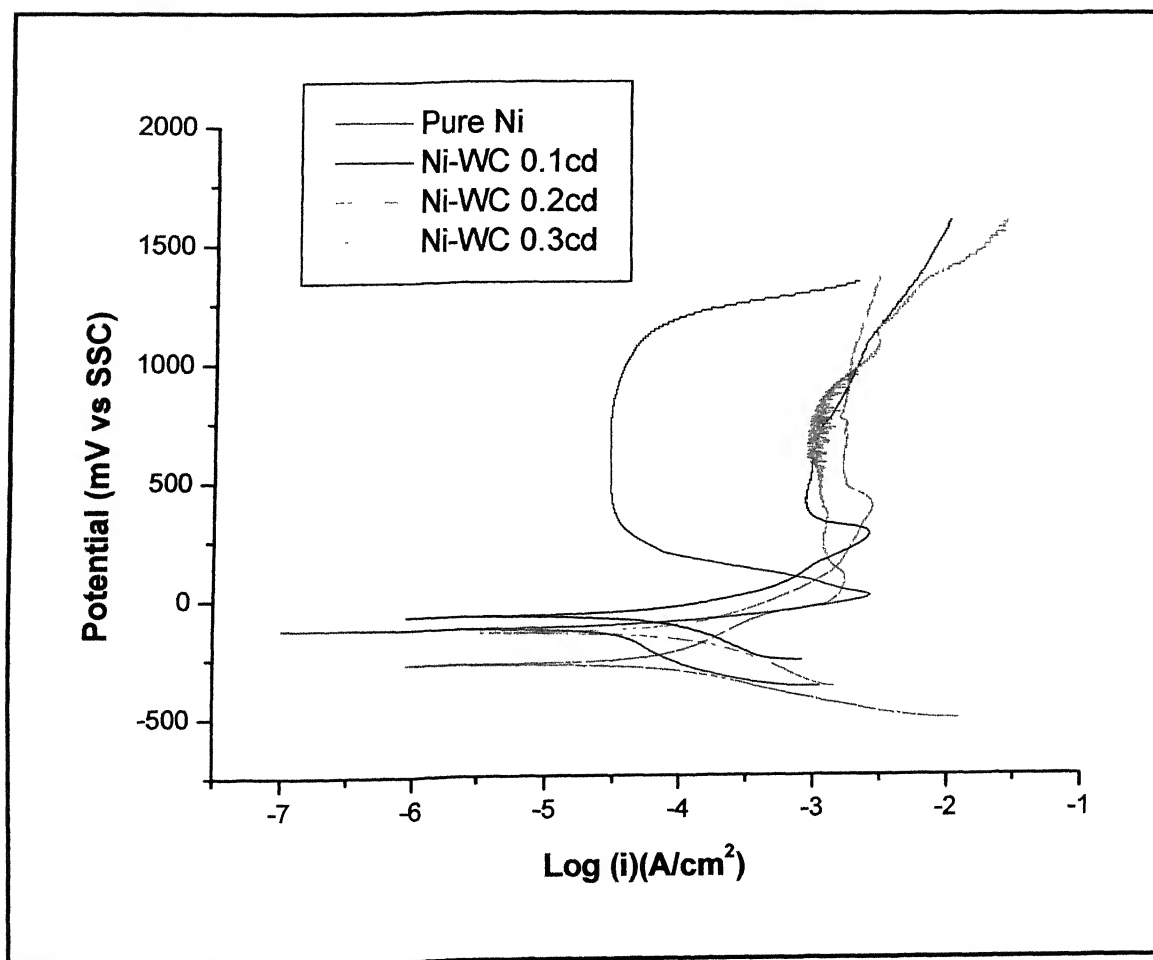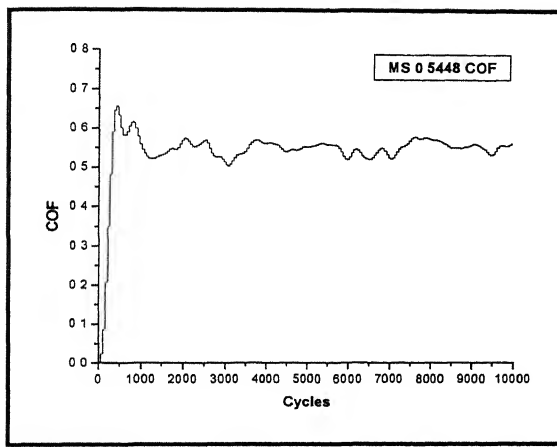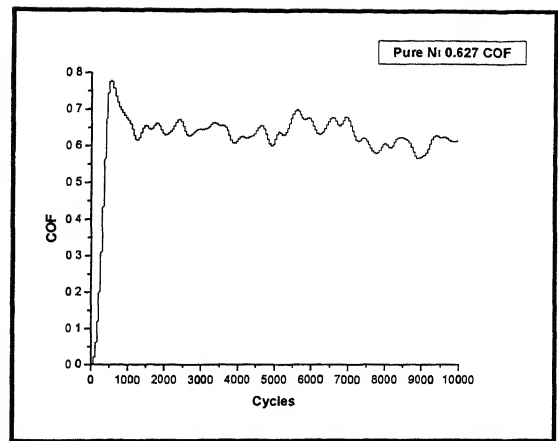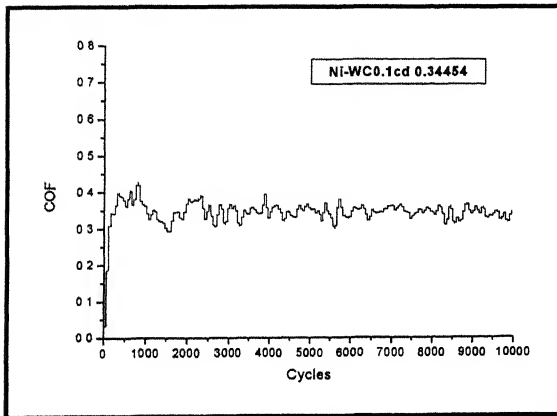| System	C.D (A/cm²)	β_c	β_a	i_{corr} (mA/cm²)	Corrosion rate (mpy)
		(V/decade)			
Pure Ni	-	-0.244	0.057	0.026	751.7213
Ni-WC	0.1	-0.233	0.129	0.074	1803.189
Ni-WC	0.2	-0.114	0.153	0.047	1250.676
Ni-WC	0.3	-0.208	0.192	0.104	2880.654

Figure 27 Potentiodynamic polarization behavior of pure Nickel and Ni-WC composite coated at different current densities.
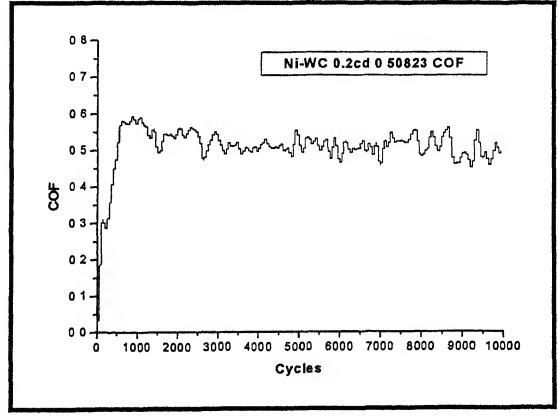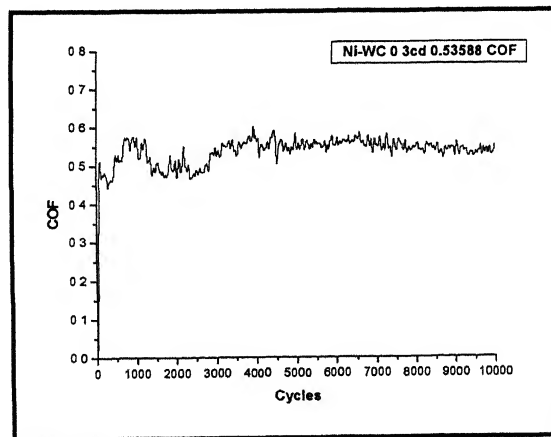
Figure 28 Coefficient of friction (COF) versus number of cycle a) mild steel b) Pure nickel c) Ni-WC 0.1 A/cm^2 c.d d) Ni-WC 0.2 A/cm^2 c.d e) Ni-WC 0.3 A/cm^2 c.d. constant testing parameters employed are 1N load, 8Hz frequency, and 100μm displacement stroke.

thereafter, COF marginally decreased and attained a steady state value within the next 1000 cycles. Comparing the steady state coefficients of friction (COF), pure nickel shows a higher value of 0.627, whereas for Ni-WC composite coating they were 0.345 at 0.1 A/cm^2 current density, 0.5082 at 0.2 A/cm^2 current density and 0.5358 at 0.3 A/cm^2 current density. Figure 29 shows the variation of COF for different systems (mild steel, pure Ni, and deposited composites at varying current densities). With increasing WC content in the deposition layer, the embedded WC particle would impede the wear process leading to lower COF when compared with pure Ni. This could be considered as a revalidation for behaviour observed in wear of electrocodeposited Ni-SiC composites, investigated by Hou et al [6] and Garcia *et al.* [65].

The coefficient of friction decreased with increasing wt% of the WC particles in the composite coating (Figure 30). Ghorbani *et al.* [64] observed that the coefficient of friction decreased with increasing graphite particles in the graphite-brass composite coating. Similar behaviour was also noted by Hou *et al.* [6], for Ni-SiC composite coating. Therefore the coefficient of friction values in the present study of Ni-WC are in agreement with published literature results for composite Ni coatings. Competition thus takes place between the beneficial increase in hardness due to reinforcing WC particles codeposited in the nickel coatings, and their adverse abrasive wear effect. The COF of metal matrix composites increases with decreasing amount of the abrasive particles, as does the hardness of the metal matrix composites.

Figure 31 shows the optical micrographs of the ultrasonically cleaned worn surfaces on the composite coatings mild steel and pure nickel, after wear against steel ball at 1 N load for 10,000 cycles. It is clearly seen from the micrographs that only some asperities had under gone wear and not the complete Hertzian contact area on the flat under the ball. However, the steel ball experienced extensive fretting wear, as revealed by the optical micrographs shown in Figure 32. The wear damage occurred on the counterbody resembles the damage on the Ni-WC coated composite flat surfaces.
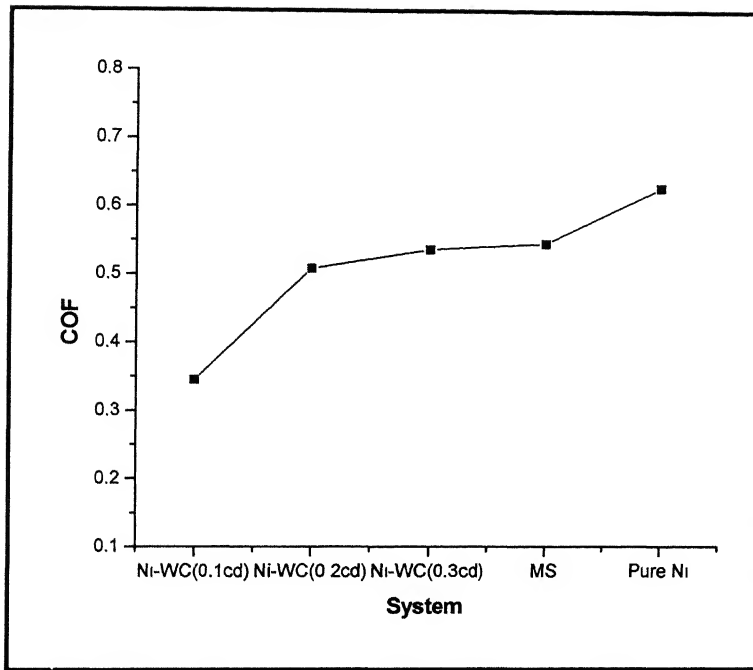
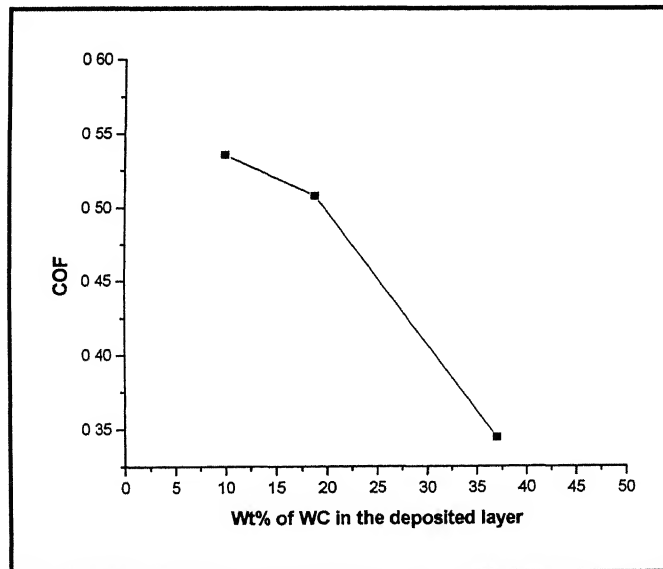Figure 29 Shows Coefficient of friction (COF) for different systems.

Figure 30 Coefficient of friction verses wt% of WC particles in the composite coating.

Figure 31 Optical micrographs of worn surfaces on Ni-WC composite coating (a) 0.1 A/cm^2 c.d (b) 0.2 A/cm^2 c.d c) 0.3 A/cm^2 c.d) Mild steel e) Pure Nickel. They were fretted against 6mm steel ball at 1N load for 10,000 cycles with a frequency of 8Hz frequency for 100μm displacement stroke. Double pointed arrows indicate the fretting direction.
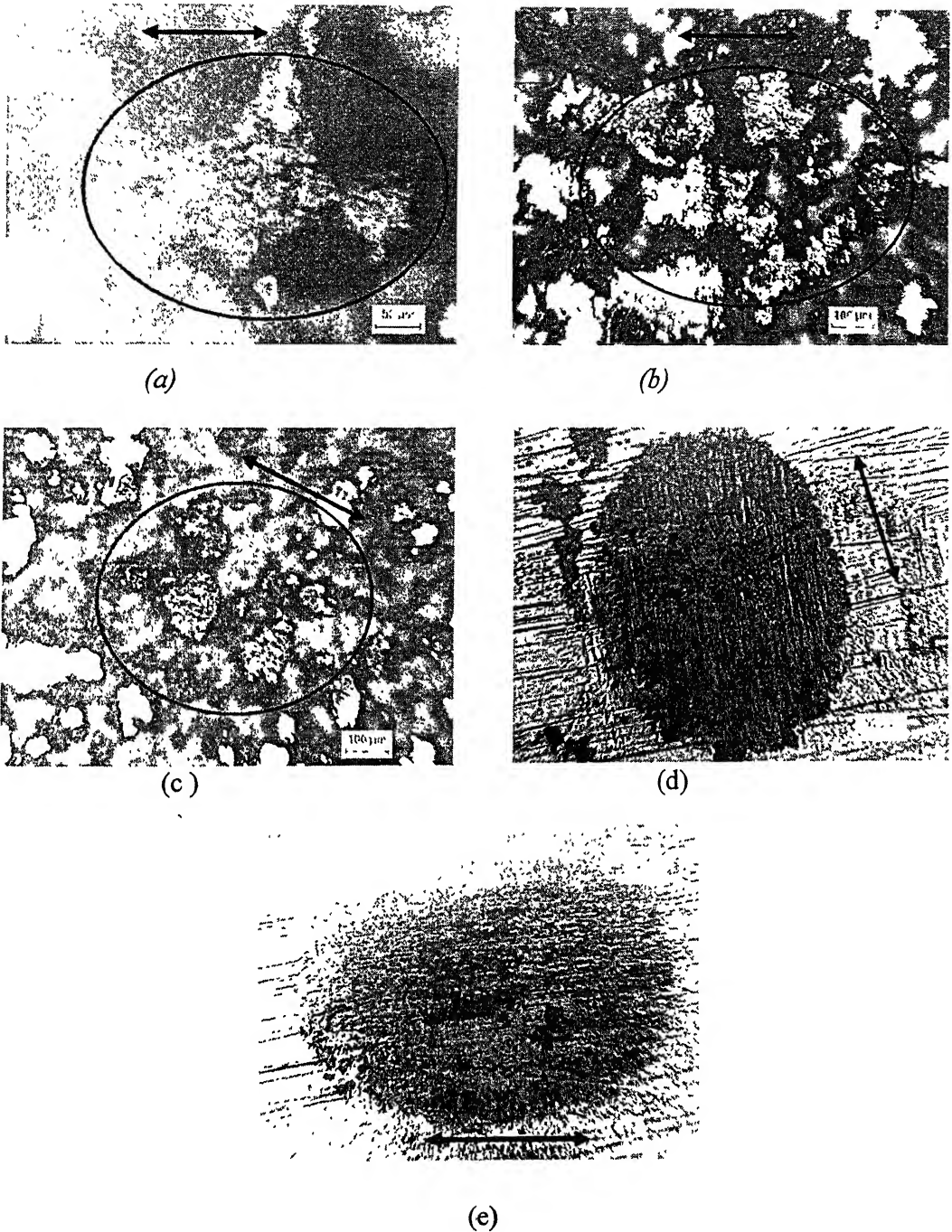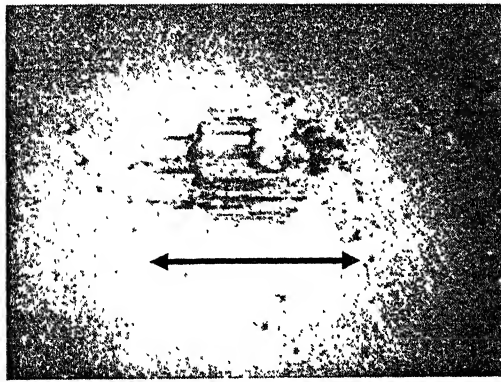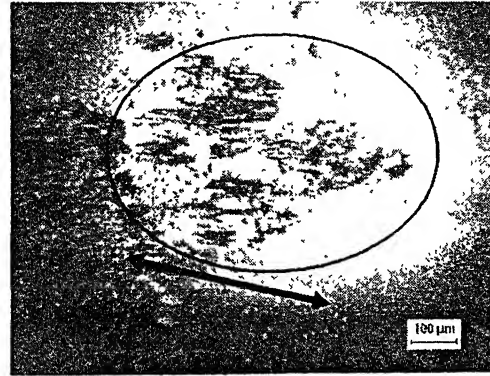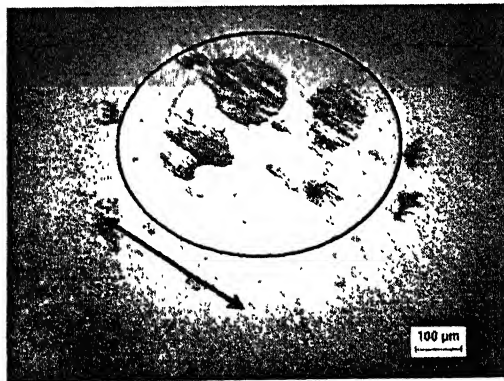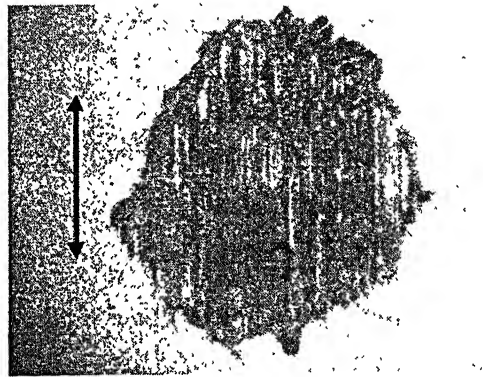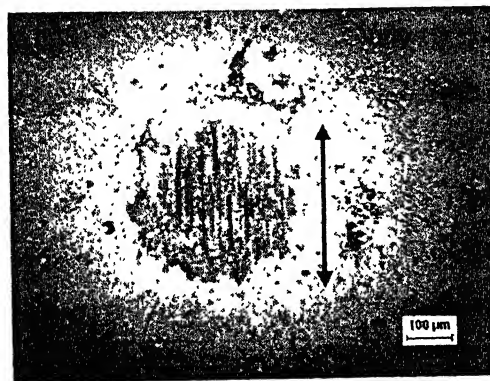
Figure 32 Optical micrographs of worn surfaces of Ni-WC composite coating a) 0.1 A/cm² c.d b) 0.2 A/cm² c.d c) 0.3 A/cm² c.d) Mild steel and e)Pure Nickel, at 1N load, 8Hz frequency for 100,000 cycles and 100μm displacement stroke. Double pointed arrows indicate the fretting direction.

Chapter 5

SUMMARY

Electrodeposited metal-matrix composite coating based on Ni-WC system has been studied in the present research. WC particles with average size of 5 μm were co-deposited with Ni using Watts' bath, with the WC particles well suspended in the electrolyte. The salient conclusions of the study and suggestions for future work are provided in this chapter.

5.1. Conclusions

- Initial studies indicated that an adherent deposit was obtained for deposition temperature above 50°C. Therefore, all further electrodeposition experiments were conducted at 50°C.

- The amount of WC in the composite increased with increasing bath load, the concentration of WC in the electrolyte. All further deposition studies were conducted using 2 g/l of WC in the electrolyte because the distribution of the carbides in the deposit layer was more uniform for this bath load. .

- The amount of WC particles in the composite coating decreased with increasing current density of deposition. This has been explained based on electrodeposition principles.

- The cathode current efficiency increased with increasing current density of deposition. This has been co-related to the increasing Ni content in the deposit.

- Optimum conditions of deposition (i.e. uniform distribution of WC and even thickness) were observed for deposition using a current density of 0.2 A/cm^2.

- The microhardness of the matrix of the composite coating increased with increasing amount of WC particles in the composite coating. The maximum value of 322 Hv was observed for deposition using a current density of 0.1 A/cm^2.

- The potentiodynamic polarization behaviour of the coated samples was compared with that of pure Ni in 0.1 mol/l sulfuric acid solution. The effect of WC carbide particles on passivation parameters was evaluated.

- The Ni-WC composite structure decreased the stability of the passive film, which was manifested by a positive shift in the passivation potential, reduction in the passive range, and higher passive current densities. The observed behaviour has been related to presence of WC in the deposit.

- The corrosion rate of the composite coatings was compared with that of Ni using polarization data. The presence of WC carbide particles increased the corrosion rate, probably due to galvanic action and localized attack due to presence of carbide particles.

- The friction and wear properties of Ni-WC composite coatings depended on the weight percentage of WC particles in the coating. The lowest co-efficient of friction (COF) against steel ball was obtained for Ni-WC composite layer deposited with 0.1 A/cm^2 current density. The COF increased with decreasing amount of WC in the deposit. The COF of pure Ni was higher compared to the composite deposits. This has been explained by the presence of WC particles in the composite.

5.2. Scope for future work

Complete suspension of WC particles in the electrolyte was difficult to achieve in the present study due to high density of WC. As uniform distribution and good deposition of second phase particles are highly effected by the suspension, the effect of surfactants on deposition can be studied.

The interfaces between Ni-WC must be related to the poorer passivation characteristics in the composites. The passivation phenomena in these composites can be understood more thoroughly by electrochemical impedance spectroscopy.

The wear behaviour should be studied in greater detail. Morphological studies are required to assess wear damage due to fretting. Investigation of large amplitude sliding wear with pin-on disk configuration can be attempted is as these coatings are used provided on flat surfaces.

References

1. S.J. Harris, *Mat. Sci. Technol.*, **4** (1988) 231.

2. J. D. Buckley, *Am. Ceram. Soc. Bull.*, **67** (2) (1988) 364.

3. J. S. Stife, and J. S. Sheehan, *Am. Ceram. Soc. Bull.*, **67** (2) (1988) 369.

4. J. Wadssworth, T. G. Nieh and J. J. Steppers, *Int. Mat. Rev.*, **33** (3) (1988) 131.

5. H. Ferkel, B. Muller and W. Riechemen, "Electrodeposition of particle strengthened nickel films," *Mater. Sci. Eng.*, **A 234** (1997) 474-476.

6. K. H. Hou, M. D. Ger, L. M. Wang and S. T. Ke, "The wear behaviour of electro-codeposited Ni-SiC composites," *Wear*, 9215 (2002) 1-10.

7. L. Benea, P. L. Bonora, A. Borello, S. Martelli, F. Wenger, P. Ponthiaux and J. Galland, "Composite eletrodeposition to obtaine nano-srtuctured coating," *J. Electrochem. Soc.*, (2001) C461-465.

8. X. H. Chen, F. Q. Cheng, S. L. Zhoa, and D. Y. Li, "Elcectrodeposited nickel composite containing carbon nanotubes," *Surf. Coat. Tech.*, **155** (2002) 247.

9. E. C. Kedward, *Metal Finish. Rev.*, (1972) 79-89.

10. M. G. Hocking, V. Vasantasree and P. S. Sidky, "Metallic and Ceramic Coatings," Longman Scientific and Technical, co-published in the United States with John Wiley and sons, Inc, New York, 1989.

11. I. Zhitomirsky, "New developments in electrolytic deposition of ceramic films," *Bull. Am. Ceram. Soc.*, **79** (2000) 57-63.

12. I. Zhitomirsky, "Cathodic electrodeposition of ceramic and organoceramic materials Fundamental aspects," *Adv. Colloid. Interface Sci.*, **97** (2002) 277-315.

13. Y. Ishikawa and Y. Matsumoto, "Electrodeposition of TiO_2 photocatalyst into nano-pores of hard alumite," *Electrochim. Acta.*, **46** (2001) 2819-2824.

14. X. Zhang, B. Yao, L. Zhao, C. Liang, L. Zhang and Y. Mao, "Electrochemical fabrication of single-crystalline anatase TiO_2 nanowire arrays," *J. Electrochem. Soc.*, **148** (2001) G398-G400.

15. T. Pauporte and D. Lincot, "Electrodeposition of semiconductors for optoelectronic devices: results on zinc oxide," *Electrochim. Acta.*, **45** (2000) 3345-3353.

16. R. Liu, A.A. Vertegel, E.W. Bohannan, T.A. Sorenson and J.A. Switzer, "Epitaxial electrodeposition of zinc oxide nanopillars on single-crystal gold," *Chem. Mater.*, **13** (2001) 508-512.

17. T. Sumida, Y. Wada, T. Kitamura and S. Yanagida, "Macroporous ZnO films electrochemically prepared by templating of opal films," *Chem. Lett.*, (2001) 38-39.

18. S.E. Hajjaji, A. Ben Bachir and L. Aries, "Electrolytic deposits on stainless steel as high temperature coatings," *Surf. Eng.*, **17** (2001) 201-204.

19. I. Zhitomirsky and A. Petric, "Electrochemical deposition of ceria and doped ceria films," *Ceram. Int.*, **27** (2001) 149-155.

20. M. Dinamani and P.V. Kamath, "Electrochemical synthesis of metal phosphates by cathodic reduction," *Mater. Res. Bull.*, **36** (2001) 2043-2050.

21. M. Manso, C. Jiménez, C. Morant, P. Herrero and J. M. Martínez-Duart, "Electrodeposition of hydroxyapatite coatings in basic conditions," *Biomaterials.*, **21** (2000) 1755-1761.

22. I. Zhitomirsky and A. Petric, "Electrolytic deposition of zirconia and zirconia organoceramic composites," *Mater. Lett.*, **46** (2000) 1-6.

23. P. Sarkar and P.S. Nicholson, "Electrophoretic deposition (EPD): Mechanisms, kinetics, and application to ceramics," *J. Am. Ceram. Soc.*, **79** (1996)1987-2002.

24. O. Van der Biest and L.J. Vandeperre, "Electrophoretic deposition of materials," *Annu. Rev. Mater. Sci.*, **29** (1999) 327-352.

25. A.T. Perez, D. Saville and C. Soria, "Modeling the electrophoretic deposition of colloidal particles," *Europhys. Lett.*, **55** (2001) 425-43.

26. P. Greil, J. Cordelair and A. Bezold, "Discrete element simulation of ceramic powder processing," *Ze. Metallk.*, **92** (2001) 682-689.

27. P. Sarkar, D. De, K. Yamashita, P.S. Nicholson and T. Umegaki, "Mimicking nanometer atomic processes on a micrometer scale via electrophoretic deposition," *J. Am. Ceram. Soc.*, **83** (2000) 1399-1401.

28. D. K. Ramanavskene, *Proc. of 10th Lithuanian Conf. of Electro Chem.*, (1968) 34-36.

29. G. A. Malone, Report No. SCL. DR, 720090, *Bell Aerospace Div.*

30. M.M. Ristic and M. K. Pavicevic, *Bull. Serbian Acad. Science Arts, Cl. Science Tech.*, **81** (20) (1982) 71-78.

31. R.S. Sayfullin, I.M. Valeyev and I. A. Abdulin, *Zasch. Met.*, **18** (2) (1982) 300-302.

32. R. Suchentinuk, *Metall.*, **35** (June 1981) 539-542.

33. R.S. Sainfullin, I. Ekkert and W.V. Bortotunov, *Zasch. Met.*, **18** (5) (1982) 792-795.

34. D. W. Snaith and P.D. Groves, *Trans. Inst. Met. Finish*, **55** (3) (1977) 136-40.

35. T. W. Tomaszewski, *Plating*, Nov. (1969) 1234-1239.

36. Devernikova and A.F. Khienoko, *Powder Metall. Met. Ceram.*, **20** (10) (Oct 1981) 726-728.

37. R.S. Saifullin and G. G. Yaminova, *Kazan Khim-Technol. Inst. Kazan, USSR deposited DOC,* 1982.

38. Tosiba Corp. Japan. Kokai, Tokyo Koho JP 59, 53, 84, 700 (cl. C251715/20) 28 Mar. 1984. Appl. 82/162, 250, 20 Sept. 199-82.

39. A. F. Krivoschchepov, A. P. Tikhhov and M. A. Lunina, *Mosk. Khim-Technol. Inst. Moscow, USSR, Zr.Prikl. Khim,* **53** (8) (1980) 1877-1879 (Russ).

40. F. A. Stott and D.J.Asby, *Corrosion Science*, **18** (1978) 183-198.

41. B.P. Cemeron, J.A. Carew and J. Foster, *10th Inst. Cong. "Metal Finishing Proceedings,"* (1980) 219-223.

42. B. Bazzard and P.J. Boden, *Trans. Inst. Metal Finishing,* **50** (2) (1972) 63-69.

43. R. J. Roos, *Trans. Inst. Metal Finish,* **55** (1977) 113-6.

44. E. A. Chassaing, *Surf. Tech.*, **7**(2) (1978)145-150.

45. E. A. Brandes and D. Goldthorpe, *Metallurgica*, (Nov. 1967) 195-198.

46. J. M. Skyes and D. J. Alner, *Trans. Inst. Met. Finish,* **52** (9) 1974.

47. N. Guglielmi, *J. Electrochem. Soc.* **119** (8) (1972) 1009-1012.

48. J. Foster and A. M. J. Kariapper, *Trans. Inst. Met. Finish.*, **51** (1973) 27-31.

49. J. P. Celis and J. R. Roos, *J. Electrchem. Soc.*, **124** (10) (1977) 1508-1511.

50. D. Prabhakaran, "Electrodeposition of Cr-WC composite coatings," *M. Tech thesis,* Indian institute of technology kanpur, 1985.

51. Rajnarayan and S. Chttopadyay, "Electrodeposited Cr-Al$_2$O$_3$ Composite coatings," *Surface. Tech.*, **16** (1982) 227-234.

52. J. P. Young, *NBSIR Rep.* 74-615, Nov 1974 (Research Directorate, Weapons loblratory, Rock Island Arsenal, IL).

53. K. R. Trethwey and J. Chamberlin, "Corrosion for Students of Science and Engineering," John Wiley & Sons, Inc., New York, 1988.

54. D. A. Jones, "Principles and Prevention of Corrosion," Maxwell Macmillan International Editions, 1992.

55. M.G. Fontana and N.D. Greene, "Corrosion Engineering," McGraw-Hill International Book Company, Japan, 2nd edition, 1983.

56. W.S. Tait, "An Introduction to Electrochemical Corrosion Testing For Practicing Engineers and Scientists," *Pair O Does Publications, Racine,* WI, USA, 1994.

57. Metals Test Methods and Analytical Procedures, Annual Book of ASTM Standards, v. 3.02, section 3, Philadelphia, PA, USA, (1987).

58. A. Brasunas and N. E. Hamner, "NACE Basic Corrosion Course", National Association of Corrosion Engineering, Houston, TX, March 11, (1970).

59. J. M. Evans and D. M. Braddick, "Corrosion behaviour of Fiber-Reinforced Al composites," *Corr. Sci.,* **11** (1971) 611-614.

60. D. M. Aylor and P. J. Moran, "Effect of reinforcement on the pitting behavior of Aluminum-base metal matrix composite," Dept. Mate. Sci. Engg, Johns Hopkins University, Baltimore, Maryland 21218.

61. M. Saxena, B. K. Prasad and T. K. Dan, "Corrosion characteristics of aluminum alloy graphite particles composite in various environments," *J. Mate. Sci.,* **27** (1992) 4805-4812.

62. B. Bhushan, "Principle and applications of Tribology," Willey Inter Science, USA., (1997).

63. R. B. Waterhouse, "Friction, Lubrication and Wear Technology-Freting wear," ASM International, Ohio, ASM Hand Book Vol.18 (1992) 242-256.

64. M.Ghorbani, M.Mazaheri, K.Khangholi and Y.Kharazi, "Electrodepostion of graphite-brass composite coatings and characterization of the tribological properties," *Surface and Coating Tech.,* **148** (2001) 71-76.

65. I.Garcai, J.Fransaer and J.P.Celis, "Electrodeopostion and sliding wear resistance of NIcomposite coatings cvontaining micron and submicron SiC particles," *Surface and Coating Tech.*, **148** (2001) 171-178.

66. J. K. Dennis and T. E. Such, "Nickel and chromium plating," Butterworth Cambridge (1986).

67. H. Mohrbacher, J. P. Celis and J. R. Roos, *Tribol. Int.*, **28** (5) (1995) 269.

68. E. Deltoumbe, N. DE Zoubov and M. Pourbaix, in Atlas of "Electrochemical Equilibrium in aqueous Solution," NACE, Houston, TX, P-330, (1974).

A145002